https://doi.org/10.5194/acp-2020-77
Preprint. Discussion started: 24 February 2020

Atmospheric Chemistry and Physics Discussions

Trends of atmospheric water vapour in Switzerland from ground-based radiometry, FTIR and GNSS data

Leonie Bernet[1,2], Elmar Brockmann[3], Thomas von Clarmann[4], Niklaus Kämpfer[1,2], Emmanuel Mahieu[5], Christian Mätzler[1,2], Gunter Stober[1,2], and Klemens Hocke[1,2]

[1]Institute of Applied Physics, University of Bern, Bern, Switzerland
[2]Oeschger Centre for Climate Change Research, University of Bern, Bern, Switzerland
[3]Federal Office of Topography, swisstopo, Wabern, Switzerland
[4]Institute of Meteorology and Climate Research, Karlsruhe Institute of Technology, Karlsruhe, Germany
[5]Institute of Astrophysics and Geophysics, University of Liège, Liège, Belgium

Correspondence: Leonie Bernet (leonie.bernet@iap.unibe.ch)

Abstract.

Vertically integrated water vapour (IWV) is expected to increase globally in a warming climate. To determine whether IWV increases as expected on a regional scale, we present IWV trends in Switzerland from ground-based remote sensing techniques and reanalysis models, considering data for the time period 1995 to 2018. We estimate IWV trends from a ground-based microwave radiometer in Bern, from a Fourier Transform Infrared (FTIR) spectrometer at Jungfraujoch, from reanalysis data (ERA5 and MERRA-2) and from Swiss ground-based Global Navigation Satellite System (GNSS) stations. Using a straightforward trend method, we account for jumps in the GNSS data, which are highly sensitive to instrumental changes. We found that IWV generally increased by 2 to $5\,\%$ per decade, with deviating trends at some GNSS stations. Trends were significantly positive at $23\,\%$ of all GNSS stations, which often lie at higher altitudes (between 850 and $1700\,\mathrm{m}$ above sea level). Our results further show that IWV in Bern scales to air temperature as expected (except in winter), but the IWV–temperature relation based on reanalysis data in whole Switzerland is not everywhere clear. In addition to our positive IWV trends, we found that the radiometer in Bern agrees within $5\,\%$ with GNSS and reanalyses. At the high altitude station Jungfraujoch, we found a mean difference of $0.26\,\mathrm{mm}$ ($15\,\%$) between the FTIR and coincident GNSS data, improving to $4\,\%$ after an antenna update in 2016. In general, we showed that ground-based GNSS data are highly valuable for climate monitoring, given that the data have been homogeneously reprocessed and that instrumental changes are accounted for. We found a response of IWV to rising temperature in Switzerland, which is relevant for projected changes in local cloud and precipitation processes.

1 Introduction

Atmospheric water vapour is a key component in the climate system. It is the most abundant greenhouse gas and responsible for a strong positive feedback that enhances temperature increase induced by other greenhouse gases (e.g. IPCC, 2013; Stocker et al., 2001). Furthermore, water vapour is involved in important tropospheric processes such as cloud formation, it builds the link between temperature and precipitation, it influences size, composition and optical properties of aerosols and it is

https://doi.org/10.5194/acp-2020-77
Preprint. Discussion started: 24 February 2020


Atmospheric Chemistry and Physics Discussions

responsible for atmospheric energy and heat transport via evaporation and condensation (Kämpfer, 2013). Measuring changes in atmospheric water vapour is thus important because they reflect externally forced temperature changes in the climate system and can be an indicator for changes in involved processes such as cloud formation and precipitation. Concentrating hereby on regional changes is of special interest, because water vapour is spatially variable and the relation between water vapour, temperature and precipitation shows spatial dependencies.

Temperature and water vapour are closely linked as expected from the Clausius-Clapeyron relation. Several studies have revealed spatial correlation between mass changes of vertically integrated water vapour (IWV) and changes in temperature, especially over oceans (e.g. Wentz and Schabel, 2000; Trenberth et al., 2005; Wang et al., 2016). Nevertheless, it has also been shown that water vapour scales not everywhere to temperature as expected and that large regional differences exist (e.g. O'Gorman and Muller, 2010; Chen and Liu, 2016; Wang et al., 2016). Over continental areas, correlations between surface temperature and IWV changes are smaller than over oceans, showing in some regions even opposite trends (Wagner et al., 2006). Also, temperature climate feedbacks may have regional dependencies (Armour et al., 2013). Regional analyses of changes in water vapour and the relation to temperature changes are thus required.

Most of the atmospheric water vapour resides in the troposphere. Measuring IWV, vertically integrated over the whole atmospheric column, is therefore representative for tropospheric water vapour. The IWV can be measured by different techniques. Nadir sounding satellite techniques provide global data sets of IWV that have been used for global trend analyses in multiple studies (e.g. Trenberth et al., 2005; Santer et al., 2007; Wentz et al., 2007; Mieruch et al., 2008; Hartmann et al., 2013; Ho et al., 2018; Zhang et al., 2018). Most of these studies found global IWV trends between 1 and 2 % per decade, with large spatial differences. However, these satellite data sets have some limitations for regional IWV trend analyses. First, missing homogenization across multiple satellite platforms can make satellite trend studies difficult (Hartmann et al., 2013; John et al., 2011). Second, many satellite products are restricted to oceans only, because the well-known ocean surface emissivity makes retrievals generally easier over oceans than over land surfaces (Urban, 2013). Stable and long-term station measurements from ground are therefore more appropriate for regional IWV trend analyses over land. From ground, IWV can be measured by radiosondes (Ross and Elliot, 2001), sun photometers (Precision Filter Radiometers (PFR), Ingold et al. (2000), Wehrli (2000)), Fourier transform infrared (FTIR) spectrometers (Sussmann et al., 2009; Schneider et al., 2012), or microwave radiometers (Morland et al., 2009). Radiosondes probably provide the longest time series, but the homogeneity of the records can be problematic due to changes in instrumentation or observational routines (Ross and Elliot, 2001) and the temporal sampling is sparse (usually twice a day). PFR and FTIR instruments measure during day and clear-sky conditions only, whereas microwave radiometers can measure in almost all weather conditions during day and night with high temporal resolution. However, no dense measurement network exist for these techniques. Another technique that provides data in all weather situations are ground-based receivers of the Global Navigation Satellite System (GNSS). The advantage of GNSS receivers is the high spatial resolution due to dense networks. In the present study we combine the microwave and FTIR techniques at two Swiss measurement stations with data from the ground-based GNSS network in Switzerland to analyse IWV trends.

Several studies use GNSS measurements to derive global IWV trends over land (e.g. Chen and Liu, 2016; Wang et al., 2016; Parracho et al., 2018). Chen and Liu (2016) report GNSS derived IWV trends at mid-latitudes of 1.46 % per decade, and

https://doi.org/10.5194/acp-2020-77
Preprint. Discussion started: 24 February 2020


Atmospheric Chemistry and Physics Discussions

Parracho et al. (2018) found IWV trends in the northern hemisphere of approximately $2.6\,\%$ per decade based on GNSS and reanalysis data. The high spatial resolution of some regional GNSS networks makes them a valuable data set for regional trend analyses of IWV. For Europe, IWV trends based on GNSS data have been presented, for example, for Germany (Alshawaf et al., 2017) and Scandinavia (Nilsson and Elgered, 2008), who observed large trend variability between different stations.

To the best of our knowledge, no regional analysis of IWV trends covering the whole area of Switzerland has been published so far. Some studies presented IWV trends at single Swiss stations (Morland et al., 2009; Sussmann et al., 2009; Hocke et al., 2011, 2016; Nyeki et al., 2019), but most of them cover shorter time periods than available today. Morland et al. (2009) and Hocke et al. (2011, 2016) presented IWV trends at Bern using the same microwave radiometer that we use in the present study. However, they use time series of maximal 13 years, whereas a time series of 24 years (1995-2018) is available now. Granted that Switzerland experienced strong warming in the last decade, an update is of particular interest. Indeed, nine of the warmest ten years in Switzerland (from 1864 to 2018) have occurred in the last two decades, and six of them lie in the last decade (NCCS, 2018). A recent study by Nyeki et al. (2019) presents GNSS based trends for longer time series (until 2015), but they concentrate only on four Swiss stations. In fact, none of the mentioned studies presents IWV trends in whole Switzerland.

Our study presents a complete trend analysis of IWV in Switzerland based on data from the Swiss GNSS station network, a microwave radiometer located in Bern, an FTIR spectrometer located at Jungfraujoch and from reanalysis models. We present IWV trends for time series of 24 years (radiometer, FTIR and reanalyses) or 19 years (GNSS) and analyse how they are related to observed changes in temperature. To avoid artificial trends, homogenized radiometer data have been used in the present study (Morland et al., 2009; Hocke et al., 2011). For the GNSS data, possible jumps due to instrumental changes have been considered in the trend analysis by using the feature of bias fitting in the trend programme of von Clarmann et al. (2010). The goal of our study is to present trends of IWV in Switzerland, to detect potential regional differences and to verify if water vapour increases as expected from the observed temperature rise.

2 Water vapour data sets

We compare IWV data from a microwave radiometer located in Bern and an FTIR spectrometer at Jungfraujoch with Swiss GNSS ground stations and reanalysis data (ERA5 and MERRA2). Radiometer data are available from 1995 onwards. We therefore define our study period from January 1995 to December 2018, even though GNSS data are available only after 2000 (see Table 1). IWV is often given as the total mass of water vapour per square metre ($\mathrm{kg\,m^{-2}}$). However, we provide IWV data in mm, taking the density of water into account, which is often referred to as "total precipitable water vapour". Evidently not all of the water vapour is actually precipitable. To avoid confusion, we prefer the term integrated water vapour (IWV) and provide the amount in the more convenient unit of mm, where $1\,\mathrm{mm}$ corresponds to $1\,\mathrm{kg\,m^{-2}}$.

2.1 Microwave radiometer

The Tropospheric Water Radiometer (TROWARA) is a microwave radiometer that has been retrieving IWV and integrated liquid water (ILW) since November 1994 in Bern, Switzerland (46.95° N, 7.44° E, 575 m above sea level (a.s.l.)). It measures

https://doi.org/10.5194/acp-2020-77
Preprint. Discussion started: 24 February 2020


Atmospheric Chemistry and Physics Discussions

the thermal emission lines of water vapour at 21.39 and 31.5 GHz with a time resolution of several seconds and an elevation angle of 40°. The measured signal is used to infer the atmospheric opacity, using the Rayleigh-Jeans approximation of the radiative transfer equation as described in Mätzler and Morland (2009) and Ingold et al. (1998).

The opacity linearly depends on the water content in the atmosphere, and can therefore be used to derive IWV and ILW (Mätzler and Morland, 2009; Hocke et al., 2017):

$$\tau_i = a_i + b_i IWV + c_i ILW, \tag{1}$$

where τ_i is the opacity of the i-th frequency channel of the radiometer. The coefficients a_i and b_i are statistically derived from nearby radiosonde measurements and fine-tuned with clear-sky measurements (Mätzler and Morland, 2009). The coefficient c_i is the Rayleigh mass absorption coefficient of liquid water.

The initial instrument setup and measurement principle is presented in Peter and Kämpfer (1992). To improve the measurement stability and data availability, the instrument was upgraded in 2002 and 2004 and a new radiometer model was developed (Morland, 2002; Morland et al., 2006). Further, it was moved into an indoor laboratory in November 2002, which made it possible to measure IWV even during light rain conditions (Morland, 2002). However, to maintain consistency with the measurements before 2002, data observed during rainy conditions were excluded in the present study as soon as the ILW exceeds 0.5 mm or rain is detected by the collocated weather station (Morland et al., 2009). TROWARA data before 2008 were harmonized (Morland et al., 2009) and data gaps before 2009 were filled with data derived from a collocated radiometer as described by Hocke et al. (2011) and Gerber (2009).

2.2 Fourier transform infrared spectrometer

A ground-based solar Fourier transform infrared (FTIR) spectrometer is located at the high altitude observatory Jungfraujoch in Switzerland (46.55° N, 7.98° E, 3580 m a.s.l.). Water vapour information is retrieved from absorption in the solar spectrum at three spectral intervals within 11.7 and 11.9 µm. The optimized IWV retrieval for FTIR spectrometry is described by Sussmann et al. (2009) and instrumental details are given in Zander et al. (2008). FTIR measurements at Jungfraujoch provide water vapour data since 1984. For consistency with our study period, we use data only from 1995 to 2018. In this period, two FTIR instruments were installed at Jungfraujoch, with overlapping measurements from 1995 to 2001. Sussmann et al. showed that the bias between both instruments is negligible. We therefore compute monthly means of a merged time series including both instruments. FTIR measurements are weather dependent (cloud-free conditions are required) and provide thus irregularly sampled data at Jungfraujoch, with on average eight measurement days per month in our study period. This sparse sampling can be problematic when calculating monthly means. We therefore apply the resampling method proposed by Wilhelm et al. (2019) when calculating monthly means of FTIR derived IWV. For this, the background IWV data are determined by fitting a seasonal model to daily IWV means. The seasonal model is given by a mean IWV_0, the first two seasonal harmonics with periods $T_n = 365.25/n$ and the fit coefficients a_n and b_n:

$$IWV(t) = IWV_0 + \sum_{n=1}^{2} \left(a_n \sin\left(\frac{2\pi}{T_n} \cdot t\right) + b_n \cos\left(\frac{2\pi}{T_n} \cdot t\right) \right). \tag{2}$$

https://doi.org/10.5194/acp-2020-77
Preprint. Discussion started: 24 February 2020


Atmospheric Chemistry and Physics Discussions

This seasonal model is fitted to the 15th of each month using a window length of 2 years. Due to the sparsity of the FTIR data, the model fit to each month provides a more robust estimate compared to the statistical monthly means, which might be based on only one or two days of observations at the beginning or end of a month that are not necessarily representative as a monthly mean. The measurement uncertainties of the obtained monthly mean values are derived from the covariance matrix of the model fit. Further, we also tested a seasonal model with higher seasonal harmonics. However, due to the sparse FTIR measurements it appeared not to be useful to improve the obtained monthly mean IWV estimates.

2.3 GNSS ground stations

The signal of GNSS satellites is delayed when passing through the atmosphere. This so called zenith total delay (ZTD) can be used to infer information about the atmospheric water vapour content. Various studies explain the method to derive IWV from the measured ZTD (e.g. Bevis et al., 1992; Hagemann et al., 2002; Guerova et al., 2003; Heise et al., 2009). We briefly summarize the procedure that we used in our study. The ZTD can be written as the sum of the zenith hydrostatic delay (ZHD) due to refraction by the dry atmosphere, and the zenith wet delay (ZWD) due to refraction by water vapour (Davis et al., 1985):

$$ZTD = ZHD + ZWD \tag{3}$$

The ZHD (in metres) is calculated from the surface pressure at each GNSS station as proposed by Elgered et al. (1991):

$$ZHD = (2.2768 \pm 0.024) \times 10^{-3} \frac{p_s}{f(\lambda, H)} \tag{4}$$

with surface pressure p_s in hPa. The dependency of the gravitational acceleration on latitude and altitude is considered in the function f (Saastamoinen, 1972):

$$f(\lambda, H) = 1 - 0.00266 \cos(2\frac{\lambda\pi}{180}) - 0.00028\,H \tag{5}$$

where λ is the station latitude in degrees and H is the station altitude in km. With the measured ZTD and the calculated ZHD, we obtain the ZWD (Eq. 3), which can then be used to infer information about the IWV in mm. It is calculated according Bevis et al. (1992) with

$$IWV = \kappa\, ZWD \frac{1}{\rho_{H_2O}} \tag{6}$$

where ρ_{H_2O} is the density of liquid water ($\rho_{H_2O} = 1000\,\mathrm{kg\,m^{-3}}$). The factor κ is given by

$$\frac{1}{\kappa} = R_v (\frac{k_3}{T_m} + k_2') 10^{-6} \tag{7}$$

with the constants k_3 and k_2' as derived by Davis et al. (1985) from Thayer (1974) ($k_3 = (3.776 \pm 0.004) \times 10^5\,\mathrm{K^2\,hPa^{-1}}$ and $k_2' = 17 \pm 10\,\mathrm{K\,hPa^{-1}}$). The required estimate of the mean atmospheric temperature T_m is linearly approximated from the surface temperature T_s (damped with the daily mean) as proposed by Bevis et al. (1992) ($T_m = 70.2\,\mathrm{K} + 0.72\,T_s$). The

https://doi.org/10.5194/acp-2020-77
Preprint. Discussion started: 24 February 2020


Atmospheric Chemistry and Physics Discussions

pressure p_s and the surface temperature T_s at the GNSS station are interpolated from pressure and temperature measurements at the closest meteorological station, assuming hydrostatic equilibrium and an adiabatic lapse rate of $6.5\,\mathrm{K\,km^{-1}}$.

We use hourly ZTD data from the Automated GNSS Network for Switzerland (AGNES), containing 41 antennas (at 31 locations), as well as data from a few stations that are part of the COGEAR network (https://mpg.igp.ethz.ch/research/geomonitoring/cogear-gnss-monitoring.html) and from two additional stations in Bern. The AGNES network has been established in 2001 (Schneider et al., 2000; Brockmann, 2001; Brockmann et al., 2001a, b) and it is maintained by the Swiss Federal Office of topography (swisstopo). A monitor web page shows the current status of all stations (Swisstopo, 2019). In 2008, most of the antennas and receivers were enhanced from GPS only to GPS and GLONASS (Russian global navigation satellite system). Since spring 2015, AGNES has been a multi-GNSS network (Brockmann et al., 2016), using data also from Galileo (European global navigation satellite system) and BeiDou (Chinese navigation satellite system). All European GNSS data were reprocessed in 2014 within the second EUREF (International Association of Geodesy Reference Frame Sub-Commission for Europe) Permanent Network (EPN) reprocessing campaign as described in Pacione et al. (2017). In the present study, only the reprocessed ZTD products of swisstopo are used (Brockmann, 2015).

The stations used in our study are shown in Fig. 1 and listed in Table 1. We only use stations that provide measurements for more than 10 years. At some GNSS stations, a new antenna and receiver were installed at the same or nearby location, replacing the older ones after an overlapping measurement period. An antenna change often leads to a small height difference, which can lead to a jump in the ZTD time series. It is therefore important to decide how to handle such instrumental changes for trend analyses. In case of antenna and receiver replacements, we merged these stations to a single time series by calculating the mean value for overlapping periods. They are marked by "_M" (for "merged") in their station abbreviation (Table 1) and a potential jump was considered in the trend estimation (see Sect. 3.1). At nine stations, new multi-GNSS receivers and antennas were installed at an additional location near-by, but the old GPS-only receivers and antennas are still operating. Swisstopo installed such twin stations to ensure a best possible long-term consistency. Simply replacing antennas at all stations would not guarantee continuous time-series, even if the phase centers of the antennas are individually calibrated. Further, no calibrations are available for the tracked satellite systems Galileo and BeiDou until today. In the case of twin stations, we only used the old, continuous GPS-only station, because the stability is better suited for trend calculations than merged time series with potential data jumps.

2.4 Reanalysis data

IWV and temperature data from two reanalysis products are used in the present study, the ERA5 and the MERRA-2 reanalyses. The Modern-Era Retrospective Analysis for Research and Applications, version 2 (MERRA-2) is an atmospheric reanalysis from NASA's Global Modeling and Assimilation Office (GMAO), described in Gelaro et al. (2017). The MERRA-2 product used in the present study for IWV data contains monthly means of vertically integrated values of water vapour (GMAO, 2015a). The product used for temperature provides monthly mean profiles (GMAO, 2015b). Both MERRA-2 products have a grid resolution of $0.5\,^\circ$ latitude $\times\, 0.625\,^\circ$ longitude. The ERA5 reanalysis is the latest atmospheric reanalysis from the European Centre for Medium Range Weather Forecasts (ECMWF) (Hersbach et al., 2018). In the present study, we use an ERA5 product

https://doi.org/10.5194/acp-2020-77
Preprint. Discussion started: 24 February 2020


Atmospheric Chemistry and Physics Discussions

providing integrated water vapour (Copernicus CDS, 2019a) and another product providing temperature profiles (Copernicus CDS, 2019b), both with a grid resolution of $0.25\,^\circ$ latitude $\times$ $0.25\,^\circ$ longitude (Copernicus Climate Change Service (C3S), 2017). Reanalysis models assume a smooth topography, that can deviate from the real topography, especially in mountainous regions (Bock et al., 2005; Bock and Parracho, 2019). For validation of reanalysis data with specific station data (e.g. GNSS), the reanalysis IWV value would need to be corrected for altitude differences as for example proposed by Bock et al. (2005) or Parracho et al. (2018). For linear trends, however, such a linear correction is not relevant. We therefore use uncorrected reanalysis data, which might lead to some differences in IWV when comparing reanalysis IWV directly with IWV measured from the radiometer or at a GNSS station.

3 Methodology

We used a multilinear parametric trend model from von Clarmann et al. (2010) to fit monthly means of IWV to the following regression function:

$$y(t) = a + b \cdot t + \sum_{n=1}^{4} \left(c_n \cdot \sin\left(\frac{2\pi t}{l_n}\right) + d_n \cdot \cos\left(\frac{2\pi t}{l_n}\right) \right) \tag{8}$$

with the estimated IWV time series $y(t)$, the time vector of monthly means t, and the fit coefficients a to d. We account for annual ($l_1 = 12$ months) and semi-annual ($l_2 = 6$ months) oscillations, as well as for two additional overtones of the annual cycle ($l_3 = 4$ months and $l_4 = 3$ months). For the FTIR trends, the solar activity is additionally fitted by using F10.7 solar flux data measured at a wavelength of $10.7\,\mathrm{cm}$ (National Research Council of Canada, 2019). Uncertainties of the time series $y(t)$ are considered in a full error covariance matrix $\mathbf{S_y}$. As uncertainties, we use the standard error of the monthly mean $\sigma_{\bar{x}} = \sigma\, n^{-\frac{1}{2}}$ (with standard deviation σ and number of measurements per month n) for TROWARA and GNSS data. FTIR uncertainties are based on the model fit of daily means as described in Sect. 2.2. For reanalysis data, we use a monthly uncertainty of 10%. This value has been chosen, because it is slightly larger than the mean relative difference of reanalysis data and TROWARA data at Bern (≈5 %). Further, it corresponds to the variability proposed by Parracho et al. (2018) for ERA-Interim and MERRA-2 that is due to model and assimilation differences.

We generally express trends in percent per decade that are derived from the regression model output in mm per decade by dividing it for each data set by its mean IWV value of the whole period. A trend is declared to be significantly different from zero at 95 % confidence interval as soon as its absolute value exceeds twice its uncertainty.

3.1 Bias fitting in the trend model

The trend model is able to consider jumps in the time series, by assuming a bias for a given subset of the data. For this, a fully correlated block is added to the part of $\mathbf{S_y}$ that corresponds to the biased subset. For each subset, the block in $\mathbf{S_y}$ is set to the square of the estimated bias uncertainty of this block. This possibility of bias fitting in the trend estimation has been presented in von Clarmann et al. (2010) and is mathematically explained in von Clarmann et al. (2001). The method has been applied for example by Eckert et al. (2014) to consider a data jump after retrieval changes in a satellite product. It is also

https://doi.org/10.5194/acp-2020-77
Preprint. Discussion started: 24 February 2020


Atmospheric Chemistry and Physics Discussions

described in Bernet et al. (2019), in which it has been applied on ozone data to consider data irregularities in a time series due to instrumental anomalies.

In the present study, we use the bias fitting on GNSS data sets to account for instrumental changes. Analysing IWV trends from GNSS data is challenging, because the measurements are highly sensitive to changes in the setup (mainly concerning antennas and radomes, but also receivers and cables) or in the environment (Pacione et al., 2017). The presented method is a straightforward way to obtain reliable IWV trend estimates despite possible data jumps due to instrumental changes. We consider each instrumental change in the trend programme, requiring as single information the dates when changes have been performed at the GNSS stations and an estimate of the bias uncertainty. We introduced change points in the trend programme as soon as antenna updates have led to a jump in the GNSS data, as recorded by swisstopo (available at http://pnac.swisstopo.admin.ch/restxt/pnac_sta.txt). After such antenna changes, we assume a bias uncertainty of 5% of the averaged IWV value for each biased subset. The bias uncertainty of $5\,\%$ has been chosen based on our example case at Neuchâtel (Fig. 2), in which we observed a bias after an antenna change of $4\,\%$. This is also consistent with results from Gradinarsky et al. (2002) and Vey et al. (2009), who found IWV jumps of around $1\,\mathrm{mm}$ due to antenna changes or changes in the number of observations and the elevation cutoff angles. For a typical Swiss station with averaged IWV values of around $16\,\mathrm{mm}$, this corresponds to a bias of around $6\,\%$. Ning et al. (2016) found IWV biases due to GNSS antenna changes mostly between 0.2 and $1\,\mathrm{mm}$, which corresponds to a bias of 1 to $6\,\%$, confirming our choice of 5 % bias uncertainty. In addition to the antenna updates, we added change points in the GNSS time series when a new receiver has been added to replace an older receiver (see Table 1). This can lead to larger biases, and we therefore assume a bias uncertainty of 10 % due to this data merging. For some antenna updates, jumps have been observed back to a data level of a previous period. These subsets have then been considered as unbiased to each other. Otherwise, we assumed the data block before the first change to be the unbiased reference block.

The trend programme and the bias correction are illustrated by an exemplary case of the GNSS station in Neuchâtel, Switzerland (Fig. 2). Figure 2a shows the monthly IWV time series of GNSS data in Neuchâtel with antenna updates in the years 2000, 2007, and 2015 (vertical red dotted lines). Figure 2b shows the deseasonalized anomalies of the IWV time series, divided by the overall mean value of each month, illustrating the interannual variability. The data variability is linked to the antenna and receiver changes, with smaller variability and less negative anomalies for the antenna used from 2007 to 2015. Furthermore, the difference to ERA5 reveals a data jump after the antenna change in 2015 (Fig. 2b). After this antenna change, the mean difference to ERA5 has been reduced, suggesting that the antenna update improved the measurements. The jump corresponds to a bias of $0.66\,\mathrm{mm}$ (4 %) compared to the data before the change. Such a jump can falsify the resulting trend. In the corrected trend fit, the trend model therefore accounts for possible biases for each antenna update. When the bias is considered in the trend model (Fig. 2c and d), we obtain a larger trend ($0.78 \pm 0.84\,\mathrm{mm}$ per decade) compared to the trend of the initial data ($0.33 \pm 0.43\,\mathrm{mm}$ per decade). In general, the trend fit (Fig. 2c) reproduces well the IWV time series. For both model fits, $90\,\%$ of the residuals (Fig. 2d) lie within $2\,\mathrm{mm}$, which corresponds to differences between observed data and model fit below 16 %. The regression model explains 93% of the variability of the IWV time series at this station.

https://doi.org/10.5194/acp-2020-77
Preprint. Discussion started: 24 February 2020


Atmospheric Chemistry and Physics Discussions

4 Integrated water vapour around Bern

IWV measurements from the TROWARA radiometer in Bern are compared to surrounding GNSS stations and reanalysis data. Figure 3 shows monthly means of TROWARA and reanalyses, as well as the averaged monthly means of seven GNSS stations close to Bern. The selected GNSS stations lie within $\pm 0.5°$ latitude and $\pm 1°$ longitude around Bern, with a maximal altitude difference of 200 m (see Table 1). The altitude restriction has been chosen to avoid the inclusion of the two higher altitude stations (Zimmerwald and Bourrignon), that are close to Bern but show larger IWV variability due to their higher elevation.

Generally, we observe a good agreement between the data sets, with interannual variability that is captured by all data sets (Fig. 3b). The data sets agree well with TROWARA, with averaged differences smaller than 0.6 mm ($\sim 5\,\%$). Only the stations in Bern (WAB1 and EXWI) show a bias compared to TROWARA (not shown). The Huttwil (HUTT) station reports less IWV than TROWARA, which is probably due to the higher station altitude. The GNSS stations around Bern agree well with TROWARA after 2013, and show larger winter differences before 2008 (Fig. 3c).

ERA5 agrees generally well with TROWARA, whereas MERRA-2 differs slightly more. Especially in the last decade, the MERRA-2 difference to TROWARA shows a strong seasonal behaviour with larger differences in winter, which is not visible in the other data sets. Correcting the reanalysis data for a possible altitude mismatch due to wrong topography assumptions (Bock and Parracho, 2019) might partly reduce discrepancies between reanalyses and observations.

4.1 IWV trends around Bern

Trends of IWV for the different data sets around Bern are shown in Fig. 4 and Table 2. IWV measured by the radiometer TROWARA increased significantly by 4.8 % per decade from 1995 to 2018. This trend value is similar to the observed trends from GNSS stations in Lausanne (EPFL), Huttwil (HUTT), Neuchâtel (NEUC) and Wabern next to Bern (WAB1), which all report trends around 5 % per decade (Fig. 4 and Table 2). We observe a slightly smaller trend in Luzern (LUZE, 3.6 % per decade) and a larger trend in Payerne (PAYE, 7.3 % per decade). The GNSS station in Bern, located at the roof of the University building of exact sciences (EXWI), shows a trend of quasi zero (0.1 % per decade). Unfortunately, the site EXWI is no longer in operation since Sept. 2017. With the exception of Payerne, all these GNSS trends are not significantly different from zero at 95% confidence interval. Reanalysis IWV at Bern increases significantly by 3.7 % per decade for MERRA-2 and by 2.3 % per decade for ERA5 data. However, the uncertainties of the monthly reanalysis data might be larger than the here used value of 10%, which would also lead to larger uncertainties of the reanalysis trends.

In brief, most of the GNSS stations around Bern report positive trends of approximately 5 % per decade (0.9 mm per decade). However, two of the GNSS stations around Bern (EXWI and PAYE) report different trends. The quasi zero trend at the EXWI station is less reliable than the other trends, because the EXWI station provides data in a shorter time period (until 2016). Further, it is not part of the AGNES network and therefore does not fulfil the same quality requirements. The large GNSS trend in Payerne results from the bias correction. If the bias correction in the trend fit (as described in Sect. 3) is not applied, the trend in Payerne is only 2 % per decade (0.32 mm per decade), whereas it increases to 7.3 % per decade (1.14 mm per decade) when accounting for antenna changes. Nyeki et al. (2019) found IWV trends in Payerne from GNSS measurements of 0.8 mm

https://doi.org/10.5194/acp-2020-77
Preprint. Discussion started: 24 February 2020


Atmospheric Chemistry and Physics Discussions

per decade, which lies between our corrected and uncorrected trends. It suggests that the instrumental changes in Payerne play an important role, but might be overcorrected in our case. The recent study of Hicks-Jalali et al. (2020) reports similar IWV trends in Payerne using nighttime radiosonde measurements (6.36 % per decade) and even larger trends using clear-night lidar data (8.85 % per decade) in the period from 2009 to 2019, suggesting that IWV in Payerne was strongly increasing, especially in recent years.

The trend from the TROWARA radiometer of 4.8 % per decade (0.72 mm per decade) slightly differs from the TROWARA trends reported by Morland et al. (2009) and Hocke et al. (2011, 2016). It is larger than TROWARA's 1996 to 2007 trend of 3.9 % per decade (0.56 mm per decade) (Morland et al., 2009). Hocke et al. (2011) found no significant TROWARA trend for the period 1994 to 2009, which suggests that our larger IWV trends are mainly due to a strong IWV increase in the last decade. This is also confirmed by Hocke et al. (2016), who observed larger trends for recent years (1.5 mm per decade for 2004 to 2015). To summarize, IWV trends around Bern from TROWARA and GNSS data generally lie around 5 % per decade, whereas reanalysis trends for the Bern grid are slightly smaller. Some GNSS stations deviate from these trend values, probably due to instrumental issues.

4.1.1 Seasonal IWV trends around Bern

To study the seasonal differences of the IWV trends around Bern, we analysed trends for each month of the year (Fig. 5). The absolute trends (Fig. 5a) are largest in summer months due to more IWV in summer. The trends in percent (Fig. 5b) account for the seasonal cycle in IWV, leading to more uniform trends throughout the year. However, differences between winter trends might sometimes be overweighted when calculating trends in percent: A small trend difference in winter will be more important when expressed in percent than the same difference in summer trends, because of less water vapour in winter. Nevertheless, we will concentrate on trends in percent per decade in the following, which facilitates comparing trends of different seasons.

Our monthly trends in Bern mostly agree on largest and significant trends in June (∼ 7 to 9 % per decade) and in November (∼ 8 to 9 % per decade) and minimal, but insignificant trends in February and October (Fig. 5b). Further, all data sets report a special pattern of low trends in October, with again larger trends in November. The mean GNSS trend agrees with the other data sets in summer, but shows an offset to the other trends in several months, especially in March and in autumn. Most of the used GNSS stations are not located within the Bern reanalysis grid, which might explain some of the trend differences. The better agreement in summer suggests that the spatial difference is less critical in summer conditions. We further found that MERRA-2 trends are slightly larger in summer than trends from the other data sets, whereas TROWARA trends differ from the other trends in the winter months December and January. This larger disagreement between TROWARA and reanalysis trends in December and January is consistent with the larger winter biases of TROWARA in Fig. 3c.

Previous studies analysed TROWARA seasonal trends using shorter time periods. Morland et al. (2009) and Hocke et al. (2011) observed significant positive summer trends and negative winter trends for TROWARA. Our TROWARA trends confirm positive summer trends (significant in June and August), but do not confirm negative winter trends. The observed autumn peak (minimum trend in October and a trend peak in November) has also been reported by Morland et al. (2009) and Hocke et al. (2011). However, their trend peak was shifted by two months, with a minimum in August and a subsequent maximum in

https://doi.org/10.5194/acp-2020-77
Preprint. Discussion started: 24 February 2020


Atmospheric Chemistry and Physics Discussions

September. The ten additional years that we use in our study compared to their data might be responsible for this shift. Morland et al. (2009) proposed that this autumn trend peak might be related to precipitation changes, but such a relationship has not been verified for the present study.

In summary, Bern data sets generally agree on the annual trend distribution, with largest trends in June and in November. However, the monthly trends of GNSS stations around Bern disagree with the other datasets in spring and in autumn, whereas TROWARA deviates in December and January. Positive summer trends are reported by all data sets.

4.2 Changes in IWV and temperature around Bern

To examine the relationship between IWV trends and changing temperature, we present the theoretical change of water vapour in the atmosphere due to observed changes in temperature (Fig. 5b). For this, we determined the temperature dependent change in saturation vapour pressure for the time period 1995 to 2018. The saturation vapour pressure e_s describes the equilibrium pressure of water between the condensed and the vapour phase. It increases rapidly with increasing temperature (Held and Soden, 2000). In case that the water vapour pressure e is smaller than e_s, the available water evaporates, whereas for $e > e_s$ it condenses until it reaches the equilibrium ($e = e_s$). With increasing temperature, e_s increases, which leads for a given e to an increase of water vapour in the vapour phase. Changes in e_s can therefore directly be compared to changes in the amount of water vapour. A required assumption is that the relative humidity (RH) remains constant,

$$RH = \frac{e}{e_s} \approx \text{constant} \tag{9}$$

so that a change in e_s is directly reflected in a change in e, and therefore in IWV:

$$\frac{de_s}{e_s} \approx \frac{de}{e} = \frac{dIWV}{IWV} \tag{10}$$

The fractional change of e_s for a given change in temperature can be approximated by the Clausius-Clapeyron equation:

$$\frac{de_s}{e_s} \approx \frac{L_v}{R_v T^2} dT \tag{11}$$

where L_v is the latent heat of evaporation ($L_v = 2.5 \times 10^6\,\mathrm{J\,kg^{-1}}$), R_v is the gas constant for water vapour ($R_v = 461\,\mathrm{J\,K^{-1}\,kg^{-1}}$), dT is the change in temperature and T is the actual temperature. To obtain the tropospheric temperature change dT, we derived the temperature trend (1995 to 2018) from MERRA-2 and ERA5 temperature profiles, averaged below $500\,\mathrm{hPa}$. This limit was chosen because 95 % of IWV resides below $500\,\mathrm{hPa}$ for the averaged MERRA-2 profiles in our study period. The resulting temperature trend (in K per decade) is then used for dT in Eq. (11) to determine the change in e_s in percent per decade. For the actual temperature T we used the mean of reanalysis temperature profiles below $500\,\mathrm{hPa}$ for the same time period.

The fractional changes in e_s for the Bern grid for different months are shown by the grey lines in Fig. 5b. These temperature induced changes in e_s agree generally well with the observed trends in IWV. They agree especially well with TROWARA and reanalysis trends in spring (March and April), late summer and autumn (July to November), and less good in the winter months and in May and June. Furthermore, they agree less with GNSS trends from September to March, which might again partly be

https://doi.org/10.5194/acp-2020-77
Preprint. Discussion started: 24 February 2020


Atmospheric Chemistry and Physics Discussions

345 explained by the spatial difference of most GNSS stations to the used reanalysis grids at Bern. Generally, the good agreement between the change in e_s and the IWV trends indicates that observed IWV changes around Bern can mostly be explained by temperature changes. However, the changes in e_s do not confirm our observed IWV winter trends, especially in January and February. This discrepancy might be related to temperature inversions that are often present in winter. In these situations, the surface water vapour is trapped by the inversion and less propagating in the free troposphere (Fujita and Sato, 2017), which 350 means that the water vapour content does not scale anymore to temperature above the inversion layer. Furthermore, other factors than temperature might be responsible for IWV changes in winter, such as changes in dynamical patterns and the horizontal transport of humid air. Indeed, Hocke et al. (2019) showed that evaporation of surface water plays a minor role in winter, with a latent heat flux that is in Bern six to seven times smaller than in summer, suggesting that horizontal transport of humid air is in winter more important than evaporation. We thus conclude that IWV in Bern changes as expected from temperature changes 355 in early spring, late summer and autumn, but other processes might also be responsible for IWV changes, especially in winter.

5 Integrated water vapour at Jungfraujoch

We compare IWV at Jungfraujoch from a GNSS antenna and an FTIR spectrometer. (Fig. 6) Due to the sparser FTIR sampling, we compare FTIR data not only with the full GNSS time series, but also with coincident GNSS data, i.e. pairwise data limited to clear-sky weather conditions. Monthly means of these sparser data have been computed by a seasonal fitting as described 360 in Sect. 2.2. This leads to some missing data at the edges of the coincident GNSS time series (Fig. 6a,c), because a specific number of data points is required for the seasonal fitting. For the FTIR time series, no data are missing at the edges because data were available beyond the dates of our study period.

We observe less IWV at Jungfraujoch than at Bern due to the high altitude of the station, with mean IWV from GNSS of $3\,\mathrm{mm}$ (Fig. 6a). The deseasonalised anomalies (Fig. 6b) show that the interannual variability of IWV at Jungfraujoch is larger 365 than in Bern, with anomalies larger than 50 % for some months. A mean bias of $-0.26 \pm 0.3\,\mathrm{mm}$ is found when comparing monthly means of coincident GNSS and FTIR measurements (Fig. 6c). This corresponds to a bias of $15\,\%$ when referring to the long-term average of GNSS coincident IWV data. Compared to the fully sampled GNSS time series, we found a bias of $1.05 \pm 0.61\,\mathrm{mm}$, which corresponds to a bias of 34 % (using the mean of the fully sampled GNSS as reference). This larger bias illustrates the sampling effect of the FTIR measurements, leading to a dry bias of FTIR compared to GNSS data. Indeed, 370 the difference results from the restriction that FTIR measurements require clear-sky conditions, preventing measurements during the wettest days. Nevertheless, the remaining bias of $-0.26\,\mathrm{mm}$ when using coincident GNSS measurements indicates that GNSS measures slightly less IWV than FTIR. This result is consistent with previous studies that reported negative GNSS biases compared to Precision Filter Radiometer (PFR) data at Jungfraujoch (Guerova et al., 2003; Haefele et al., 2004; Nyeki et al., 2005; Morland et al., 2006). Guerova et al. attributed this bias to incorrect modelling of the antenna phase centre and 375 Haefele et al. to unmodeled multi-path effects of the Jungfraujoch antenna. Brockmann et al. (2019) stated that the old GPS-only antenna used at Jungfraujoch till 2016 was never calibrated. Due to the special radome construction (with circulating warm air to avoid icing), the standard antenna phase center calibration is not appropriate to be used with the Jungfraujoch data.

https://doi.org/10.5194/acp-2020-77
Preprint. Discussion started: 24 February 2020


Atmospheric Chemistry and Physics Discussions

From this point of view the achieved results are astonishingly good. For trend analyses, a possible offsets is not relevant as long as it is constant over the whole trend period. The use of this antenna was stopped in summer 2015 and it was replaced by a new multi-GNNS antenna in October 2016 (Brockmann et al., 2016). Furthermore, the complete antenna-radome construction was individually calibrated for GPS and GLONASS signals (Galileo and BeiDou are assumed to be identical to GPS). We found that the bias to FTIR has been reduced to $-0.07\,\mathrm{mm} \pm 0.28\,(4\,\%)$ after the antenna change in 2016, suggesting that the GNSS antenna update improved the measurements at Jungfraujoch.

5.1 IWV trends at Jungfraujoch

The IWV trends at the Jungfraujoch station from FTIR and fully sampled GNSS data are presented in Fig. 7. The GNSS antenna update has been considered in the trend estimate as described in Sect. 3.1. We observe IWV trends of $0.08\,\mathrm{mm}$ per decade ($2.8\,\%$ per decade) for GNSS and $0.04\,\mathrm{mm}$ per decade ($1.8\,\%$ per decade) for FTIR. However, both trends are insignificant. The difference between both trends might partly be explained by the dry sampling bias of the FTIR spectrometer, that measures only during clear-sky day conditions. Our IWV trends at Jungfraujoch are similar to the trend by Sussmann et al. (2009), who reported insignificant FTIR trends at the same station of $0.08\,\mathrm{mm}$ per decade in the time period 1996 to 2008. In contrast to these results, Nyeki et al. (2019) found larger trends at Jungfraujoch that were significantly different from zero. They decided not to use GNSS IWV data from Jungfraujoch due to the high IWV variability and problems due to the influence of snow and ice. Therefore, they derived their trends from IWV data based on a parameterisation from surface temperature and relative humidity measurements. However, they admit that this approximation is prone to large uncertainties (Gubler et al., 2012), which might explain parts of the differences to our trends.

6 IWV trends in Switzerland

6.1 Swiss GNSS trends

The GNSS data generally report positive IWV trends throughout Switzerland (Fig. 8). Using data for the whole year (Fig. 8a), $50\,\%$ of the stations show trends between 2.6 and $5.4\,\%$ per decade (0.30 and $0.73\,\mathrm{mm}$ per decade). The trends of all stations range between $0.1\,\%$ per decade ($0.02\,\mathrm{mm}$ per decade) and $7.3\,\%$ per decade ($1.14\,\mathrm{mm}$ per decade), with exception of three stations that show negative trends (ANDE, HOHT and MART_M). The mean trend value of all GNSS stations is $3.7\,\%$ per decade ($0.49\,\mathrm{mm}$ per decade) and the median is $4.0\,\%$ per decade ($0.57\,\mathrm{mm}$ per decade).

Only four stations ($11\,\%$ of all stations) show negative IWV trends and none of them is significantly different from zero at 95 % confidence interval. Significant positive trends are reported at 23 % percent of the stations (eight stations), being generally stations with long time series and lying mostly in western and south eastern Switzerland. Most significant trends are observed in summer (Fig. 8d), with significant positive trends at five stations. In winter, only the three north-eastern Swiss station trends are significant (Fig. 8b). In spring (Fig. 8c) and autmun (Fig. 8e), none of the IWV trends are significantly different from zero.

https://doi.org/10.5194/acp-2020-77
Preprint. Discussion started: 24 February 2020


Atmospheric Chemistry and Physics Discussions

Autumn trends tend to be negative, especially in the southwestern part (Rhône valley in the canton of Valais), but they are all insignificant.

Our trend range covered by all GNSS stations is consistent with results from Nilsson and Elgered (2008), who observed in Sweden and Finland IWV trends between -0.2 and 1 mm per decade. However, they concluded that their study period was too short (10 years) to obtain stable trends. Our trends also lie within the range of trends observed in Germany by Alshawaf et al. (2017). Their trends vary even more between different stations, with trends ranging between -1.5 to $2.3\,\mathrm{mm}$ per decade. The recent study of Nyeki et al. (2019) reports IWV trends from GNSS data at three Swiss stations for the period 2001 to 2015. Using Sen's slope trend method, they found positive all-sky trends in Davos ($0.89\,\mathrm{mm}$ per decade), Locarno ($0.42\,\mathrm{mm}$ per decade) and Payerne ($0.80\,\mathrm{mm}$ per decade). Our GNSS trends for these stations are slightly different (Davos: $0.71\,\mathrm{mm}$ per decade, Locarno: $0.69\,\mathrm{mm}$ per decade, Payerne: $1.14\,\mathrm{mm}$ per decade), which might be due to the three additional years in our analysis, but also due to our bias correction in the trend model. Furthermore, our GNSS data were reprocessed till 2014 (see Sect. 2.3), whereas Nyeki et al. still used the old GNSS-derived ZTD data.

The altitude dependence of the GNSS trends is shown in Fig. 9. We observe that most of the stations that show significant positive trends lie at higher altitudes (Fig. 9). Indeed, 88% of the stations that show significant trends lie at altitudes above $850\,\mathrm{m}$ a.s.l, whereas less than half of the stations lie above $850\,\mathrm{m}$. This is consistent with the expectation of Pepin et al. (2015) that the rate of warming is larger at higher altitudes. Due to the direct link between temperature and water vapour content, an increased warming at higher altitudes would lead to larger IWV trends. The increasing significance with altitude provides some observational evidence for this suggestion. However, the altitude dependence is less visible in absolute trends (not shown), which indicates that due to less IWV at higher altitudes, these trends are more sensitive to changes when calculating trends in percent. Also, the IWV trends of the five stations with highest altitudes ($> 1700\,\mathrm{m}$ a.s.l) are not significantly different from zero.

We conclude that Swiss GNSS stations generally show positive IWV trends, with a mean value of $3.4\,\%$ per decade ($0.44\,\mathrm{mm}$ per decade) and a tendency for more significant percentage trends at higher altitudes.

6.2 Swiss reanalysis trends

Reanalysis trends of IWV for Switzerland are presented in Fig. 10 and Fig. 11. The trends are on average $2.6\,\%$ per decade ($0.35\,\mathrm{mm}$ per decade) for ERA5 (Fig. 10a) and $3.6\,\%$ per decade ($0.52\,\mathrm{mm}$ per decade) for MERRA-2 (Fig. 11a). Both reanalysis trends show only small spatial variability. The seasonal trends are positive, with largest values in summer (Fig. 10d and 11d). This is consistent with our observed GNSS trends, which are mostly positive in summer. Smallest and partly negative reanalysis trends are observed in winter (Fig. 10b and 11b), which contrasts with our GNSS trends that showed smallest (but insignificant) trends in autumn and not in winter. In spring and autumn, the reanalysis trends are spatially more variable. Both data sets report slightly larger autumn trends in south-eastern Switzerland and northern Italy (Fig. 10e and 11e). In spring, ERA5 shows larger IWV trends in south-western Switzerland.

Our mean ERA5 trend for Switzerland of $0.35\,\mathrm{mm}$ per decade is consistent with IWV trends from ERA-Interim in Germany reported by Alshawaf et al. (2017) ($0.34\,\mathrm{mm}$ per decade). The MERRA-2 trends are generally slightly larger than the ERA5

https://doi.org/10.5194/acp-2020-77
Preprint. Discussion started: 24 February 2020


Atmospheric Chemistry and Physics Discussions

trends. Parracho et al. (2018) also found larger IWV trends for MERRA-2 compared to ERA-Interim reanalysis trends on a global scale, especially in summer. Our MERRA-2 trend (3.6 % per decade) agrees with our averaged GNSS trend (3.4 % per decade), which is slightly larger than the averaged ERA5 trend (2.6 % per decade). However, the reanalyses do not resolve small scale variability, which can explain the differences to some GNSS station trends. Alshawaf et al. (2017) also observed larger differences in mountainous regions between GNSS derived IWV trends and reanalyses in Germany.

To determine the relationship between temperature changes and IWV trends for whole Switzerland, we present changes in saturation vapour pressure e_s derived from reanalysis temperature changes below 500 hPa (as described in Sect. 4.2). The fractional change in e_s, which corresponds to the change in IWV (Eq. 10) is presented for ERA5 (Fig. 12) and for MERRA-2 (Fig. 13). The averaged changes in e_s of 2.9 % per decade (ERA5) and 4.0 % per decade (MERRA-2) are similar to our reanalysis IWV trends described before, which indicates that IWV is on average following the temperature change as expected from the Clausius-Clapeyron equation. The ERA5 e_s changes are spatially more uniform than the ERA5 IWV trends, but agree well in all seasons, except in winter (Fig. 12b and 10b). This indicates that other factors than temperature might dominate IWV changes in winter, as already discussed in Sect. 4.2. In contrast to ERA5, The MERRA-2 changes in e_s show large spatial variability, with strong differences between different grids and generally larger values in the Alpine region. On regional scales, the MERRA-2 e_s trends (Fig. 13) thus differ strongly from the MERRA-2 IWV trends (Fig. 11), especially in summer and in winter. The partly negative winter changes in e_s are surprising, because they result from a decrease in reanalysis winter temperature. Such a decrease in winter temperature is controversial to long-term temperature observations in Switzerland, that report a temperature increase also in winter (Begert and Frei, 2018). This difference is probably due to our short study period. A few cold winters in the past 15 years might have hidden the overall positive temperature trend when looking only at the relatively short period from 1995 to 2018 (MeteoSwiss, 2019).

In general, we should be careful to draw conclusions from the reanalysis trends because of their uncertainties. Due to changes in observing systems of the assimilated data, the use of reanalyses for trend studies has been debated (e.g. Bengtsson et al., 2004; Sherwood et al., 2010; Dee et al., 2011; Parracho et al., 2018). This problem has been addressed in the recent reanalysis products. Compared to the previous ECMWF reanalysis (ERA-Interim), the bias correction of assimilated data in ERA5 has been extended to more observation systems (Hersbach et al., 2018). Also MERRA-2 has been improved compared to the previous MERRA data, for example with reduced biases in the water cycle (Gelaro et al., 2017). Further analyses would be required to conclude if biases due to changes in observing systems still exist in the reanalysis data over Switzerland.

To summarize, the reanalysis IWV trends follow on average the changes expected from temperature changes, but MERRA-2 shows large regional variability for changes in e_s based on lower tropospheric temperature changes. The reanalysis IWV trends generally agree well with GNSS trends in Switzerland, but the spatial trend variability is not resolved by the reanalyses. Local measurements of IWV such as microwave radiometer, FTIR or GNSS measurements are therefore crucial to monitor changes in IWV, especially in mountainous regions such as Switzerland.

https://doi.org/10.5194/acp-2020-77
Preprint. Discussion started: 24 February 2020


Atmospheric Chemistry and Physics Discussions

7 Conclusions

Our study presents trends of integrated water vapour (IWV) in Switzerland from a ground-based microwave radiometer, an FTIR spectrometer, GNSS stations and reanalysis data. We found that IWV generally increased by around 2 to 5 % per decade in the last 24 years. Using a straightforward trend approach that accounts for jumps due to instrumental changes, we found significant positive IWV trends for some GNSS stations in western and eastern Switzerland. Further, our data show that trend significance tends to be larger in summer and to increase with altitude (up to 1700 m a.s.l.).

Comparing IWV from the radiometer in Bern with GNSS and reanalyses showed a good agreement, with differences within 5 %. The FTIR spectrometer at the high altitude station Jungfraujoch revealed a constant clear-sky bias of 1 mm compared to GNSS data. Nevertheless, both data sets agree within their uncertainties when only coincident measurements are used. We further found that the GNSS trends agree on average with the Swiss reanalysis trends, but the reanalyses are not able to capture regional variability, especially in the Alps. We conclude that GNSS data are reliable for the detection of climatic IWV trends. However, a few stations may require further quality control and harmonisation in the trend analysis.

Measurements in Bern reveal that the IWV trends follow observed temperature changes according to the Clausius-Clapeyron equation. Still, they do not scale to temperature as expected in some months, especially in winter, suggesting that other processes such as changes in dynamical patterns are responsible for IWV changes in winter. However, these winter trends are not significantly different from zero, which hinders us drawing robust conclusions about temperature related IWV changes in winter. Also, several colder winters in our study period might hide the long-term winter temperature increase in Switzerland. Nevertheless, ERA5 confirms the departure from Clausius-Clapeyron scaling in winter during our study period. This is not observed in MERRA-2 temperature data, which is spatially variable and resulting IWV changes disagree with the observed MERRA-2 IWV trends. This might be related to the poorly resolved topography in the larger MERRA-2 grids. The reanalysis grids probably miss regional variability in atmospheric stratification and convection, as it was also observed for zonal means by Wentz and Schabel (2000).

It would be necessary to analyse temperature induced changes at more stations to draw robust conclusions about correlations between temperature and IWV changes. The problem of hidden long-term temperature trends in our study might be solved by using longer temperature time series, but longer IWV time series are sparse. Comparing regional IWV changes with tropospheric temperature changes from observations (e.g. radiosondes) rather than from reanalyses might be another approach to improve understanding of regional temperature–IWV relations. Nevertheless, it is generally difficult to attribute observed climate changes to unambiguous sources and feedbacks (Santer et al., 2007). Only complex attribution studies with multiple model runs can clarify this issue, as done for example by Santer et al. (2007) for IWV over oceans. However, global climate models lack feedbacks on the regional level (Sherwood et al., 2010), and studies based on regional observations are thus necessary.

Another reason for observed inconsistencies between temperature and IWV changes might be changes in relative humidity. Our temperature–IWV relation assumes that the relative humidity remains constant. However, this is not always the case, because of limited moisture availability over land surfaces (Wang et al., 2016). Some studies found even a decrease of relative

https://doi.org/10.5194/acp-2020-77
Preprint. Discussion started: 24 February 2020


Atmospheric Chemistry and Physics Discussions

humidity with increasing temperature at midlatitudes (O'Gorman and Muller, 2010) or in the subtropics (Dessler et al., 2008). Analysing local changes of relative humidity throughout the troposphere would be necessary to examine this assumption.

In summary, our results confirm the increase of water vapour with global warming on a regional scale, stressing the importance of the water vapour feedback. Further, the results emphasise the importance of regional IWV analyses, by showing that regional trend differences can be large, especially in mountainous areas. The spatial coverage of long-term IWV measurements from ground stations is sparse. We have shown that homogeneously reprocessed GNSS data have the potential to fill this gap and that they enable monitoring of regional water vapour trends in a changing climate. We further found that water vapour increase follows temperature changes as expected, but the relationship is not everywhere clear. In a changing climate, it is therefore important to assess both, regional changes in temperature and water vapour, to understand and project possible changes in precipitation patterns and cloud formation on a regional scale.

Data availability. TROWARA and GNSS-derived IWV data are provided by the STARTWAVE database (http://www.iapmw.unibe.ch/research/projects/STARTWAVE/). The Jungfraujoch FTIR data are publicly available from the Network for the Detection of Atmospheric Composition Change (NDACC) at ftp://ftp.cpc.ncep.noaa.gov/ndacc/station/jungfrau/hdf/ftir/. MERRA2 data are available online through the NASA Goddard Earth Sciences Data Information Services Center (GES DISC) at https://disc.gsfc.nasa.gov/datasets?keywords=%22MERRA-2%22&page=1&source=Models%2FAnalyses%20MERRA-2. ERA5 data are available through the Copernicus Climate Change Service Climate Data Store (CDS) at https://cds.climate.copernicus.eu/cdsapp#!/home.

Author contributions. The study concept has been designed by LB and KH. LB analysed the data and prepared the manuscript. TvC provided the trend programme and GS provided the monthly resampling programme. EM was responsible for the FTIR data, EB for the GNSS data, and CM, NK and KH for the TROWARA data. All Co-Authors contributed to the manuscript preparation and the interpretation of the results.

Competing interests. The authors declare that they have no competing interests.

Acknowledgements. L. Bernet was funded by the Swiss National Science Foundation, grant number 200021-165516. We thank the technicians and engineers from the Institute of Applied Physics, University of Bern, who have kept TROWARA working since many years. The University of Liège's involvement has primarily been supported by the F.R.S. – FNRS (Fonds de la Recherche Scientifique) and the Belgian Federal Science Policy Office (BELSPO), both in Brussels, as well as by the GAW-CH programme of MeteoSwiss. The Fédération Wallonie Bruxelles contributed to supporting observational activities. E. Mahieu is a Research Associate with the F.R.S. – FNRS. We thank the International Foundation High Altitude Research Stations Jungfraujoch and Gornergrat (HFSJG, Bern) for supporting the facilities needed to perform the FTIR observations and the many colleagues who contributed to FTIR data acquisition at that site. The 10.7cm solar radio flux

https://doi.org/10.5194/acp-2020-77
Preprint. Discussion started: 24 February 2020

Atmospheric Chemistry and Physics Discussions

data were provided as a service by the National Research Council of Canada and distributed in partnership with Natural Resources Canada. E. Brockmann from swisstopo provided the GNSS-derived ZTD data (operationally and reprocessed) for all Swiss stations.

https://doi.org/10.5194/acp-2020-77
Preprint. Discussion started: 24 February 2020

Atmospheric Chemistry and Physics Discussions

References

Alshawaf, F., Balidakis, K., Dick, G., Heise, S., and Wickert, J.: Estimating trends in atmospheric water vapor and temperature time series over Germany, Atmos. Meas. Tech., 10, 3117–3132, https://doi.org/10.5194/amt-10-3117-2017, 2017.

Armour, K. C., Bitz, C. M., and Roe, G. H.: Time-Varying Climate Sensitivity from Regional Feedbacks, J. Clim., 26, 4518–4534, https://doi.org/10.1175/JCLI-D-12-00544.1, 2013.

Begert, M. and Frei, C.: Long-term area-mean temperature series for Switzerland—Combining homogenized station data and high resolution grid data, Int. J. Climatol., 38, 2792–2807, https://doi.org/10.1002/joc.5460, 2018.

Bengtsson, L., Hagemann, S., and Hodges, K. I.: Can climate trends be calculated from reanalysis data?, J. Geophys. Res. D Atmos., 109, D11 111, https://doi.org/10.1029/2004JD004536, 2004.

Bernet, L., von Clarmann, T., Godin-beekmann, S., Ancellet, G., and Maillard Barras, E.: Ground-based ozone profiles over central Europe: incorporating anomalous observations into the analysis of stratospheric ozone trends, Atmos. Chem. Phys., 19, 4289–4309, https://doi.org/10.5194/acp-19-4289-2019, 2019.

Bevis, M., Businger, S., Herring, T. A., Rocken, C., Anthes, R. A., and Ware, R. H.: GPS meteorology: Remote sensing of atmospheric water vapor using the global positioning system, J. Geophys. Res., 97, 15 787–15 801, https://doi.org/10.1029/92JD01517, 1992.

Bock, O. and Parracho, A. C.: Consistency and representativeness of integrated water vapour from ground-based GPS observations and ERA-Interim reanalysis, Atmos. Chem. Phys., 19, 9453–9468, https://doi.org/10.5194/acp-2019-28, 2019.

Bock, O., Keil, C., Richard, E., Flamant, C., and Bouin, M. N.: Validation for precipitable water from ECMWF model analyses with GPS and radiosonde data during the MAP SOP, Q. J. R. Meteorol. Soc., 131, 3013–3036, https://doi.org/10.1256/qj.05.27, 2005.

Brockmann, E.: Positionierungsdienste und Geodaten des Schweizerischen Bundesamtes für Landestopographie, in: Tagungsband - POSNAV 2001, DGON-Symposium Positionierung und Navig. 6. bis 8. März 2001, Dresden, DGON, Bonn, 2001.

Brockmann, E.: Reprocessed GNSS tropospheric products at swisstopo, GNSS4SWEC workshop, Thessaloniki, May 11-14 2015, 2015.

Brockmann, E., Grünig, S., Hug, R., Schneider, D., Wiget, A., and Wild, U.: National Report of Switzerland Introduction and first applications of a Real-Time Precise Positioning Service using the Swiss Permanent Network, in: Subcomm. Eur. Ref. Fram. (EUREF). EUREF Publ. No. 10, edited by Torres, J. and Hornik, H., pp. 272–276, Mitteilungen des Bundesamtes für Kartographie und Geodäsie, Vol. 23, Frankfurt am Main 2002, http://www.euref.eu/symposia/book2001/nr%5C_28.PDF, 2001a.

Brockmann, E., Guerova, G., and Troller, M.: Swiss Activities in Combining GPS with Meteorology, in: Subcommission for the European Reference Frame (EUREF). EUREF Publication No. 10, edited by Torres, J. and Hornik, H., pp. 95–99, Mitteilungen des Bundesamtes für Kartographie und Geodäsie, Vol. 23, Frankfurt am Main 2002, http://www.euref.eu/symposia/book2001/2_6.pdf, 2001b.

Brockmann, E., Andrey, D., Ineichen, D., Kislig, L., Liechti, J., Lutz, S., Misslin, C., Schaer, S., and Wild, U.: Automated GNSS Network Switzerland (AGNES), International Foundation HFSJG, Activity Report 2016, https://www.hfsjg.ch/wordpress/reports/2016/137_Swisstopo_Brockmann.pdf, 2016.

Brockmann, E., Andrey, D., Ineichen, D., Lutz, S., Wild, U., Vapor, I. W., and Delay, Z. P.: Automated GNSS Network Switzerland (AGNES), International Foundation HFSJG, Activity Report 2019, 2019.

Chen, B. and Liu, Z.: Global water vapor variability and trend from the latest 36 year (1979 to 2014) data of ECMWF and NCEP reanalyses, radiosonde, GPS, and microwave satellite, J. Geophys. Res., 121, 11 442–11 462, https://doi.org/10.1002/2016JD024917, 2016.

Copernicus CDS: ERA5 monthly averaged data on single levels from 1979 to present, https://cds.climate.copernicus.eu/cdsapp#!/dataset/reanalysis-era5-single-levels-monthly-means?tab=overview, 2019a.

https://doi.org/10.5194/acp-2020-77
Preprint. Discussion started: 24 February 2020

Atmospheric Chemistry and Physics Discussions

Copernicus CDS: ERA5 monthly averaged data on pressure levels from 1979 to present, https://cds.climate.copernicus.eu/cdsapp#!/dataset/reanalysis-era5-pressure-levels-monthly-means?tab=overview, 2019b.

Copernicus Climate Change Service (C3S): ERA5: Fifth generation of ECMWF atmospheric reanalyses of the global climate, https://cds.climate.copernicus.eu/cdsapp#!/home, 2017.

Davis, J. L., Herrinch, T. A., Shapiro, I. I., Rogers, A. E. E., and Elgered, G.: Geodesy by radio interferometry: Effects of atmospheric modeling errors on estimates of baseline length, Radio Sci., 20, 1593–1607, 1985.

Dee, D. P., Uppala, S. M., Simmons, A. J., Berrisford, P., Poli, P., Kobayashi, S., Andrae, U., Balmaseda, M. A., Balsamo, G., Bauer, P., Bechtold, P., Beljaars, A. C., van de Berg, L., Bidlot, J., Bormann, N., Delsol, C., Dragani, R., Fuentes, M., Geer, A. J., Haimberger, L., Healy, S. B., Hersbach, H., Hólm, E. V., Isaksen, L., Kållberg, P., Köhler, M., Matricardi, M., Mcnally, A. P., Monge-Sanz, B. M., Morcrette, J. J., Park, B. K., Peubey, C., de Rosnay, P., Tavolato, C., Thépaut, J. N., and Vitart, F.: The ERA-Interim reanalysis: Configuration and performance of the data assimilation system, Q. J. R. Meteorol. Soc., 137, 553–597, https://doi.org/10.1002/qj.828, 2011.

Dessler, A. E., Yang, P., Lee, J., Solbrig, J., Zhang, Z., and Minschwaner, K.: An analysis of the dependence of clear-sky top-of-atmosphere outgoing longwave radiation on atmospheric temperature and water vapor, J. Geophys. Res., 113, D17 102, https://doi.org/10.1029/2008JD010137, 2008.

Eckert, E., von Clarmann, T., Kiefer, M., Stiller, G. P., Lossow, S., Glatthor, N., Degenstein, D. A., Froidevaux, L., Godin-Beekmann, S., Leblanc, T., McDermid, S., Pastel, M., Steinbrecht, W., Swart, D. P. J., Walker, K. A., and Bernath, P. F.: Drift-corrected trends and periodic variations in MIPAS IMK/IAA ozone measurements, Atmos. Chem. Phys., 14, 2571–2589, https://doi.org/10.5194/acp-14-2571-2014, 2014.

Elgered, G., Davis, J. L., Herring, T. A., and Shapiro, I. I.: Geodesy by Radio Interferometry: Water Vapor Radiometry for Estimation of the Wet Delay, J. Geophys. Res., 96, 6541–6555, 1991.

Fujita, M. and Sato, T.: Observed behaviours of precipitable water vapour and precipitation intensity in response to upper air profiles estimated from surface air temperature, Sci. Rep., 7, 5–10, https://doi.org/10.1038/s41598-017-04443-9, 2017.

Gelaro, R., McCarty, W., Suárez, M. J., Todling, R., Molod, A., Takacs, L., Randles, C. A., Darmenov, A., Bosilovich, M. G., Reichle, R., Wargan, K., Coy, L., Cullather, R., Draper, C., Akella, S., Buchard, V., Conaty, A., da Silva, A. M., Gu, W., Kim, G. K., Koster, R., Lucchesi, R., Merkova, D., Nielsen, J. E., Partyka, G., Pawson, S., Putman, W., Rienecker, M., Schubert, S. D., Sienkiewicz, M., and Zhao, B.: The Modern-Era Retrospective Analysis for Research and Applications, version 2 (MERRA-2), J. Clim., 30, 5419–5454, https://doi.org/10.1175/JCLI-D-16-0758.1, 2017.

Gerber, C.: Combining measurements from the microwave radiometers TROWARA and GROMOS for improved trend analysis of the integrated water vapour, Bachelor thesis, University of Bern, 2009.

Global Modeling and Assimilation Office (GMAO): MERRA-2 instM_2d_int_Nx: 2d, Monthly mean, Instantaneous, Single-Level, Assimilation, Vertically Integrated Diagnostics V5.12.4, Goddard Earth Sciences Data and Information Services Center (GES DISC), Greenbelt, MD, USA, https://doi.org/10.5067/KVTU1A8BWFSJ, 2015a.

Global Modeling and Assimilation Office (GMAO): MERRA-2 instM_3d_asm_Np: 3d, Monthly mean, Instantaneous, Pressure-Level, Assimilation, Assimilated Meteorological Fields V5.12.4, Goddard Earth Sciences Data and Information Services Center (GES DISC), Greenbelt, MD, USA, https://doi.org/10.5067/2E096JV59PK7, 2015b.

Gradinarsky, L. P., Johansson, J. M., Bouma, H. R., Scherneck, H. G., and Elgered, G.: Climate monitoring using GPS, Phys. Chem. Earth, 27, 335–340, https://doi.org/10.1016/S1474-7065(02)00009-8, 2002.

https://doi.org/10.5194/acp-2020-77
Preprint. Discussion started: 24 February 2020

Atmospheric Chemistry and Physics Discussions

Gubler, S., Gruber, S., and Purves, R. S.: Uncertainties of parameterized surface downward clear-sky shortwave and all-sky longwave radiation, Atmos. Chem. Phys., 12, 5077–5098, https://doi.org/10.5194/acp-12-5077-2012, 2012.

Guerova, G., Brockmann, E., Quiby, J., Schubiger, F., and Mätzler, C.: Validation of NWP Mesoscale Models with Swiss GPS Network AGNES, J. Appl. Meteorol., 42, 141–150, https://doi.org/10.1175/1520-0450(2003)042<0141:vonmmw>2.0.co;2, 2003.

Haefele, P., Martin, L., Becker, M., Brockmann, E., Morland, J., Nyeki, S., Mätzler, C., and Kirchner, M.: Impact of radiometrie water vapor measurements on troposphere and height estimates by GPS, in: Proc. 17th Int. Tech. Meet. Satell. Div. Inst. Navig. ION GNSS 2004, pp. 2289–2302, Long Beach, CA, 2004.

Hagemann, S., Bengtsson, L., and Gendt, G.: On the determination of atmospheric water vapour from GPS measurements, Tech. Rep. 340, Max Planck Institute for Meteorology, Hamburg, Germany, 2002.

Hartmann, D., Tank, A. K., Rusticucci, M., Alexander, L., Brönnimann, S., Charabi, Y., Dentener, F., Dlugokencky, E., Easterling, D., Kaplan, A., Soden, B., Thorne, P., Wild, M., and P.M. Zhai: Observations: Atmosphere and Surface, in: Climate Change 2013: The Physical Science Basis. Contribution of Working Group I to the Fifth Assessment Report of the Intergovernmental Panel on Climate Change, edited by Stocker, T., Qin, D., Plattner, G.-K., Tignor, M., Allen, S., Boschung, J., Nauels, A., Xia, Y., Bex, V., and Midgley, P., chap. 2, pp. 159–254, Cambridge University Press, Cambridge, https://doi.org/10.1017/CBO9781107415324.008, 2013.

Heise, S., Dick, G., Gendt, G., Schmidt, T., and Wickert, J.: Integrated water vapor from IGS ground-based GPS observations: Initial results from a global 5-min data set, Ann. Geophys., 27, 2851–2859, https://doi.org/10.5194/angeo-27-2851-2009, 2009.

Held, I. M. and Soden, B. J.: Water Vapor Feedback and Global Warming, Annu. Rev. Energy Environ., 25, 441–475, 2000.

Hersbach, H., De Rosnay, P., Bell, B., Schepers, D., Simmons, A., Soci, C., Abdalla, S., Balmaseda, A., Balsamo, G., Bechtold, P., Berrisford, P., Bidlot, J., De Boisséson, E., Bonavita, M., Browne, P., Buizza, R., Dahlgren, P., Dee, D., Dragani, R., Diamantakis, M., Flemming, J., Forbes, R., Geer, A., Haiden, T., Hólm, E., Haimberger, L., Hogan, R., Horányi, A., Janisková, M., Laloyaux, P., Lopez, P., Muñoz-Sabater, J., Peubey, C., Radu, R., Richardson, D., Thépaut, J.-N., Vitart, F., Yang, X., Zsótér, E., and Zuo, H.: Operational global reanalysis: progress, future directions and synergies with NWP including updates on the ERA5 production status, in: ERA Rep. Ser. No. 27, European Centre for Medium Range Weather Forecasts (ECMWF), Reading, England, https://doi.org/10.21957/tkic6g3wm, 2018.

Hicks-Jalali, S., Sica, R. J., Haefele, A., Martucci, G., Maillard Barras, E., and Voirin, J.: A Raman Lidar Tropospheric Water Vapour Climatology and Height-Resolved Trend Analysis over Payerne Switzerland, Atmos. Chem. Phys. Discuss., pp. 1–29, https://doi.org/10.5194/acp-2019-1089, 2020.

Ho, S. P., Peng, L., Mears, C., and Anthes, R. A.: Comparison of global observations and trends of total precipitable water derived from microwave radiometers and COSMIC radio occultation from 2006 to 2013, Atmos. Chem. Phys., 18, 259–274, https://doi.org/10.5194/acp-18-259-2018, 2018.

Hocke, K., Kämpfer, N., Gerber, C., and Mätzler, C.: A complete long-term series of integrated water vapour from ground-based microwave radiometers, Int. J. Remote Sens., 32, 751–765, https://doi.org/10.1080/01431161.2010.517792, 2011.

Hocke, K., Navas Guzmán, F., Cossu, F., and Mätzler, C.: Cloud Fraction of Liquid Water Clouds above Switzerland over the Last 12 Years, Climate, 4, 48, https://doi.org/10.3390/cli4040048, http://www.mdpi.com/2225-1154/4/4/48, 2016.

Hocke, K., Navas-Guzmán, F., Moreira, L., Bernet, L., and Mätzler, C.: Oscillations in atmospheric water above Switzerland, Atmos. Chem. Phys., 17, 12 121–12 131, https://doi.org/10.5194/acp-17-12121-2017, 2017.

Hocke, K., Bernet, L., Hagen, J., Murk, A., Renker, M., and Mätzler, C.: Diurnal cycle of short-term fluctuations of integrated water vapour above Switzerland, Atmos. Chem. Phys., 19, 12 083–12 090, https://doi.org/10.5194/acp-19-12083-2019, 2019.

https://doi.org/10.5194/acp-2020-77
Preprint. Discussion started: 24 February 2020

Atmospheric Chemistry and Physics Discussions

Ingold, T., Peter, R., and Kämpfer, N.: Weighted mean tropospheric temperature and transmittance determination at millimeter-wave frequencies for ground-based applications, Radio Sci., 33, 905–918, https://doi.org/10.1002/zaac.200400263, 1998.

Ingold, T., Schmid, B., Mätzler, C., Demoulin, P., and Kämpfer, N.: Modeled and empirical approaches for retrieving columnar water vapor from solar tranmittance measurements in the 0.72, 0.82, and 0.94 μm absorption bands, J. Geophys. Res., 105, 24 327–24 343, 2000.

IPCC: Summary for Policymakers, in: Climate Change 2013: The Physical Science Basis. Contribution of Working Group I to the Fifth Assessment Report of the Intergovernmental Panel on Climate Change, edited by Stocker, T., Qin, D., Plattner, G.-K., Tignor, M., Allen, S., Boschung, J., Nauels, A., Xia, Y., Bex, V., and Midgley, P., Cambridge University Press, Cambridge, United Kingdom and New York, NY, USA, https://doi.org/10.1017/CBO9781107415324.004, 2013.

John, V. O., Holl, G., Allan, R. P., Buehler, S. A., Parker, D. E., and Soden, B. J.: Clear-sky biases in satellite infrared estimates of upper tropospheric humidity and its trends, J. Geophys. Res. Atmos., 116, D14 108, https://doi.org/10.1029/2010JD015355, 2011.

Kämpfer, N.: Introduction, in: Monitoring Atmospheric Water Vapour. Ground-based Remote Sensing and In-situ Methods, edited by Kämpfer, N., chap. 1, pp. 1–7, Springer New York, New York, NY, https://doi.org/10.1007/978-1-4614-3909-7_1, 2013.

Mätzler, C. and Morland, J.: Refined physical retrieval of integrated water vapor and cloud liquid for microwave radiometer data, IEEE Trans. Geosci. Remote Sens., 47, 1585–1594, https://doi.org/10.1109/TGRS.2008.2006984, 2009.

MeteoSwiss (Federal Institute for Meteorology and Climatology): Temperature and precipitation trends, https://www.meteoswiss.admin.ch/home/climate/climate-change-in-switzerland/temperature-and-precipitation-trends.html?filters=ths200m0_swiss_djf_1864-smoother, 2019.

Mieruch, S., Noël, S., Bovensmann, H., and Burrows, J. P.: Analysis of global water vapour trends from satellite measurements in the visible spectral range, Atmos. Chem. Phys., 8, 491–504, https://doi.org/10.5194/acp-8-491-2008, 2008.

Morland, J.: TROWARA - Tropospheric Water Vapour Radiometer. Radiometer review and new calibration model ., Tech. rep., University of Bern, Bern, Switzerland, 2002.

Morland, J., Deuber, B., Feist, D. G., Martin, L., Nyeki, S., Kämpfer, N., Mätzler, C., Jeannet, P., and Vuilleumier, L.: The STARTWAVE atmospheric water database, Atmos. Chem. Phys., 6, 2039–2056, www.atmos-chem-phys.net/6/2039/2006/, 2006.

Morland, J., Coen, C. M., Hocke, K., Jeannet, P., and Mätzler, C.: Tropospheric water vapour above Switzerland over the last 12 years, Atmos. Chem. Phys., 9, 5975–5988, https://doi.org/10.5194/acp-9-5975-2009, 2009.

National Research Council of Canada: Latest Solar Radio Flux Report from DRAO, Penticton, https://www.spaceweather.gc.ca/solarflux/sx-5-mavg-en.php, 2019.

NCCS: CH2018 – Climate Scenarios for Switzerland, p. 271, Technical Report, National Centre for Climate Services, Zurich, 2018.

Nilsson, T. and Elgered, G.: Long-term trends in the atmospheric water vapor content estimated from ground-based GPS data, J. Geophys. Res. Atmos., 113, https://doi.org/10.1029/2008JD010110, 2008.

Ning, T., Wickert, J., Deng, Z., Heise, S., Dick, G., Vey, S., and Schöne, T.: Homogenized time series of the atmospheric water vapor content obtained from the GNSS reprocessed data, J. Clim., 29, 2443–2456, https://doi.org/10.1175/JCLI-D-15-0158.1, 2016.

Nyeki, S., Vuilleumier, L., Morland, J., Bokoye, A., Viatte, P., Mätzler, C., and Kämpfer, N.: A 10-year integrated atmospheric water vapor record using precision filter radiometers at two high-alpine sites, Geophys. Res. Lett., 32, L23 803, https://doi.org/10.1029/2005GL024079, 2005.

Nyeki, S., Wacker, S., Aebi, C., Gröbner, J., Martucci, G., and Vuilleumier, L.: Trends in surface radiation and cloud radiative effect at four Swiss sites for the 1996–2015 period, Atmos. Chem. Phys., 19, 13 227–13 241, https://doi.org/10.5194/acp-19-13227-2019, 2019.

https://doi.org/10.5194/acp-2020-77
Preprint. Discussion started: 24 February 2020

Atmospheric Chemistry and Physics Discussions

O'Gorman, P. A. and Muller, C. J.: How closely do changes in surface and column water vapor follow Clausius-Clapeyron scaling in climate change simulations?, Environ. Res. Lett., 5, https://doi.org/10.1088/1748-9326/5/2/025207, 2010.

Pacione, R., Araszkiewicz, A., Brockmann, E., and Dousa, J.: EPN-Repro2: A reference GNSS tropospheric data set over Europe, Atmos. Meas. Tech., 10, 1689–1705, https://doi.org/10.5194/amt-10-1689-2017, 2017.

Parracho, A. C., Bock, O., and Bastin, S.: Global IWV trends and variability in atmospheric reanalyses and GPS observations, Atmos. Chem. Phys., 18, 16 213–16 237, https://doi.org/10.5194/acp-18-16213-2018, 2018.

Pepin, N., Bradley, R. S., Diaz, H. F., Baraer, M., Caceres, E. B., Forsythe, N., Fowler, H., Greenwood, G., Hashmi, M. Z., Liu, X. D., Miller, J. R., Ning, L., Ohmura, A., Palazzi, E., Rangwala, I., Schöner, W., Severskiy, I., Shahgedanova, M., Wang, M. B., Williamson, S. N., and Yang, D. Q.: Elevation-dependent warming in mountain regions of the world, Nat. Clim. Chang., 5, 424–430, https://doi.org/10.1038/nclimate2563, 2015.

Peter, R. and Kämpfer, N.: Radiometric Determination of Water Vapor and Liquid Water and Its Validation With Other Techniques, J. Geophys. Res., 97, 18 173–18 183, 1992.

Ross, R. J. and Elliot, W. P.: Radiosonde-based Northern Hemisphere tropospheric water vapor trends, J. Clim., 14, 1602–1612, https://doi.org/10.1175/1520-0442(2001)014<1602:RBNHTW>2.0.CO;2, 2001.

Saastamoinen, J.: Atmospheric Correction for the Troposphere and Stratosphere in Radio Ranging Satellites, in: Use Artif. Satell. Geod., edited by S. W. Henriksen et al., vol. 15, pp. 247–251, Geophys. Monogr. Ser., Washington, D.C., https://doi.org/10.1029/GM015p0247, 1972.

Santer, B. D., Mears, C., Wentz, F. J., Taylor, K. E., Gleckler, P. J., Wigley, T. M. L., Barnett, T. P., Boyle, J. S., Bruggemann, W., Gillett, N. P., Klein, S. A., Meehl, G. A., Nozawa, T., Pierce, D. W., Stott, P. A., Washington, W. M., and Wehner, M. F.: Identification of human-induced changes in atmospheric moisture content, Proc. Natl. Acad. Sci., 104, 15 248–15 253, https://doi.org/10.1073/pnas.0702872104, 2007.

Schneider, D., Brockmann, E., Marti, U., Schlatter, A., and Wild, U.: National Report of Switzerland Introduction of a Precise Swiss Positioning Service "swipos" and Progress in the Swiss National Height Network " LHN95 ", in: Rep. Symp. IAG Subcomm. Eur. held Tromsø, 22 - 24 June 2000, edited by Torres, J., pp. 315–322, 2000.

Schneider, M., Barthlott, S., Hase, F., González, Y., Yoshimura, K., García, O. E., Sepúlveda, E., Gomez-Pelaez, A., Gisi, M., Kohlhepp, R., Dohe, S., Blumenstock, T., Wiegele, A., Christner, E., Strong, K., Weaver, D., Palm, M., Deutscher, N. M., Warneke, T., Notholt, J., Lejeune, B., Demoulin, P., Jones, N., Griffith, D. W., Smale, D., and Robinson, J.: Ground-based remote sensing of tropospheric water vapour isotopologues within the project MUSICA, Atmos. Meas. Tech., 5, 3007–3027, https://doi.org/10.5194/amt-5-3007-2012, 2012.

Sherwood, S. C., Roca, R., Weckwerth, T. M., and Andronova, N. G.: Tropospheric water vapor, convection, and climate, Rev. Geophys., 48, RG2001, https://doi.org/10.1029/2009RG000301, 2010.

Stocker, T. F., Clarke, G., Treut, H. L., Lindzen, R., Meleshko, V., Mugara, R., Palmer, T., Pierrehumbert, R., Sellers, P., Trenberth, K., and Willebrand, J.: Physical Climate Processes and Feedbacks, in: Climate Change 2001: The Scientific Basis. Contribution of Working Group I to the Third Assessment Report of the Intergovernmental Panel on Climate Change, edited by Houghton, J., Ding, Y., Griggs, D., Noguer, M., van der Linden, P., Dai, X., Maskell, K., and Johnson, C., chap. 7, pp. 417–470, Cambridge University Press, Cambridge, United Kingdom and New York, NY, USA,, 2001.

Sussmann, R., Borsdorff, T., Rettinger, M., Camy-Peyret, C., Demoulin, P., Duchatelet, P., Mahieu, E., and Servais, C.: Technical Note: Harmonized retrieval of column-integrated atmospheric water vapor from the FTIR network – First examples for long-term records and station trends, Atmos. Chem. Phys., 9, 8987–8999, https://doi.org/10.5194/acp-9-8987-2009, 2009.

https://doi.org/10.5194/acp-2020-77
Preprint. Discussion started: 24 February 2020

Atmospheric Chemistry and Physics Discussions

Swisstopo: Automated GNSS Network for Switzerland (AGNES), http://pnac.swisstopo.admin.ch/pages/en/agnes.html, 2019.

Thayer, G. D.: An improved equation for the radio refractive index of air, Radio Sci., 9, 803–807, https://doi.org/10.1029/RS009i010p00803, 1974.

Trenberth, K. E., Fasullo, J., and Smith, L.: Trends and variability in column-integrated atmospheric water vapor, Clim. Dyn., 24, 741–758, https://doi.org/10.1007/s00382-005-0017-4, 2005.

Urban, J.: Satellite Sensors Measuring Atmospheric Water Vapour, in: Monitoring Atmospheric Water Vapour. Ground-based Remote Sensing and In-situ Methods, edited by Kämpfer, N., chap. 9, pp. 175–214, Springer New York, New York, NY, https://doi.org/10.1007/978-1-4614-3909-7, 2013.

Vey, S., Dietrich, R., Fritsche, M., Rülke, A., Steigenberger, P., and Rothacher, M.: On the homogeneity and interpretation of precipitable water time series derived from global GPS observations, J. Geophys. Res. Atmos., 114, D10 101, https://doi.org/10.1029/2008JD010415, 2009.

von Clarmann, T., Grabowski, U., and Kiefer, M.: On the role of non-random errors in inverse problems in radiative transfer and other applications, J. Quant. Spectrosc. Radiat. Transf., 71, 39–46, https://doi.org/10.1016/S0022-4073(01)00010-3, 2001.

von Clarmann, T., Stiller, G. P., Grabowski, U., Eckert, E., and Orphal, J.: Technical note: Trend estimation from irregularly sampled, correlated data, Atmos. Chem. Phys., 10, 6737–6747, https://doi.org/10.5194/acp-10-6737-2010, 2010.

Wagner, T., Beirle, S., Grzegorski, M., and Platt, U.: Global trends (1996-2003) of total column precipitable water observed by Global Ozone Monitoring Experiment (GOME) on ERS-2 and their relation to near-surface temperature, J. Geophys. Res. Atmos., 111, D12 102, https://doi.org/10.1029/2005JD006523, 2006.

Wang, J., Dai, A., and Mears, C.: Global water vapor trend from 1988 to 2011 and its diurnal asymmetry based on GPS, radiosonde, and microwave satellite measurements, J. Clim., 29, 5205–5222, https://doi.org/10.1175/JCLI-D-15-0485.1, 2016.

Wehrli, C.: Calibrations of filter radiometers for determination of atmospheric optical depth, Metrologia, 37, 419–422, https://doi.org/10.1088/0026-1394/37/5/16, 2000.

Wentz, F. J. and Schabel, M.: Precise climate monitoring using complementary satellite data sets, Nature, 403, 414–416, https://doi.org/10.1038/35000184, 2000.

Wentz, F. J., Ricciardulli, L., Hilburn, K., and Mears, C.: How much more rain will global warming bring?, Science (80-.)., 317, 233–235, https://doi.org/10.1126/science.1140746, 2007.

Wilhelm, S., Stober, G., and Brown, P.: Climatologies and long-term changes in mesospheric wind and wave measurements based on radar observations at high and mid latitudes, Ann. Geophys., 37, 851–875, https://doi.org/10.5194/angeo-37-851-2019, 2019.

Zander, R., Mahieu, E., Demoulin, P., Duchatelet, P., Roland, G., Servais, C., Mazière, M. D., Reimann, S., and Rinsland, C. P.: Our changing atmosphere: Evidence based on long-term infrared solar observations at the Jungfraujoch since 1950, Sci. Total Environ., 391, 184–195, https://doi.org/10.1016/j.scitotenv.2007.10.018, 2008.

Zhang, Y., Xu, J., Yang, N., and Lan, P.: Variability and Trends in Global Precipitable Water Vapor Retrieved from COSMIC Radio Occultation and Radiosonde Observations, Atmosphere (Basel)., 9, https://doi.org/10.3390/atmos9050174, 2018.

https://doi.org/10.5194/acp-2020-77
Preprint. Discussion started: 24 February 2020

Atmospheric Chemistry and Physics Discussions

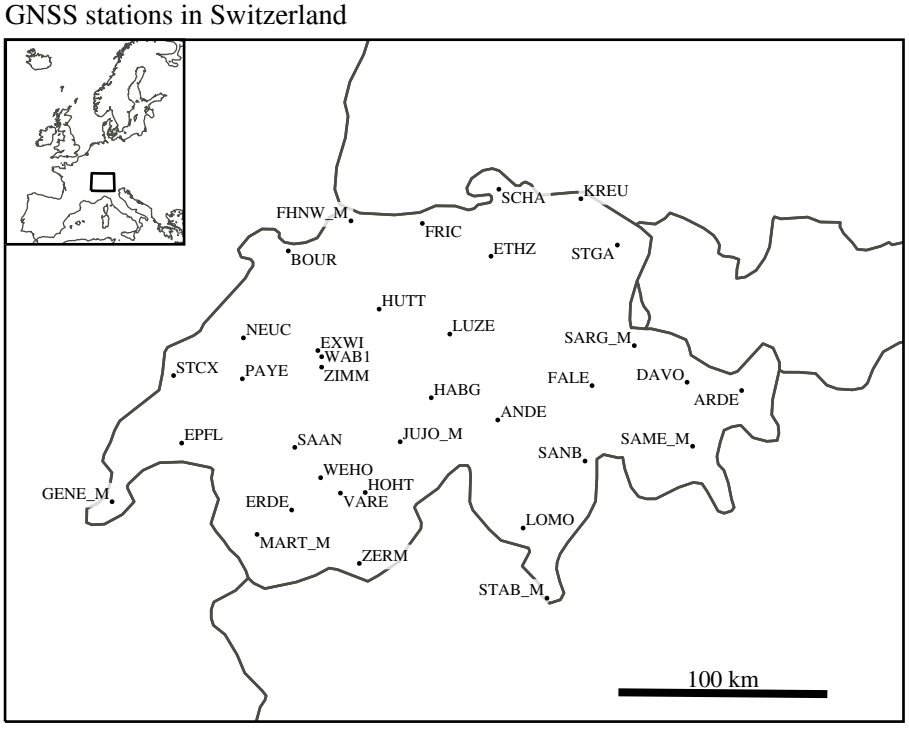

Figure 1. Map of Swiss Global Navigation Satellite System (GNSS) stations used in this study.

https://doi.org/10.5194/acp-2020-77
Preprint. Discussion started: 24 February 2020

Atmospheric Chemistry and Physics Discussions

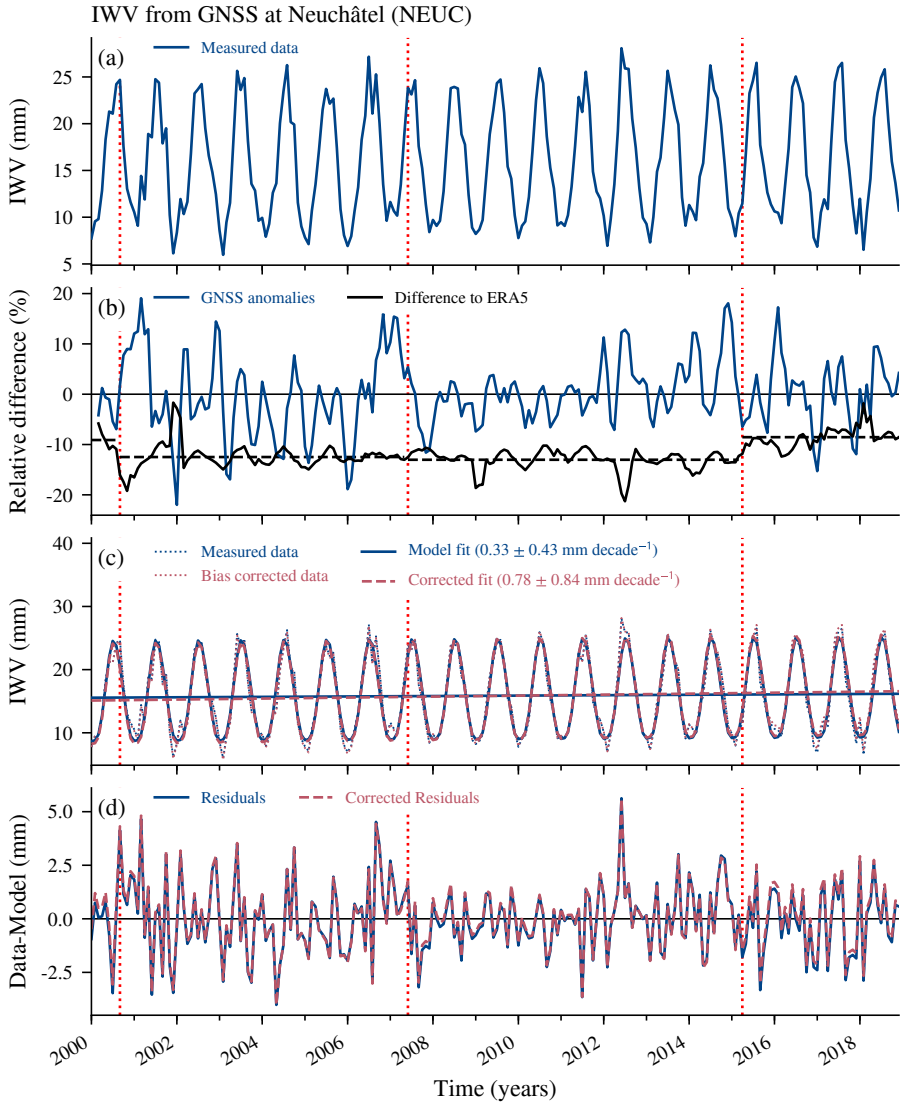

Figure 2. **(a)** Monthly means of integrated water vapour (IWV) from the GNSS station at Neuchâtel (NEUC), Switzerland. Changes in antenna and receiver types are indicated in all panels by vertical red dotted lines. **(b)** Anomalies from the climatology ((data−climatology)/climatology) of the GNSS data at Neuchâtel and relative difference to ERA5 data at the same location ((ERA5−GNSS)/GNSS), both smoothed with a three-months moving window. The horizontal black dashed lines show the averaged difference to ERA5 for each antenna change. **(c)** Regression model fit and **(d)** residuals of the model with and without considering data jumps in the trend model. The given trend uncertainties correspond to 2 standard deviations (σ).

https://doi.org/10.5194/acp-2020-77
Preprint. Discussion started: 24 February 2020

Atmospheric Chemistry and Physics Discussions

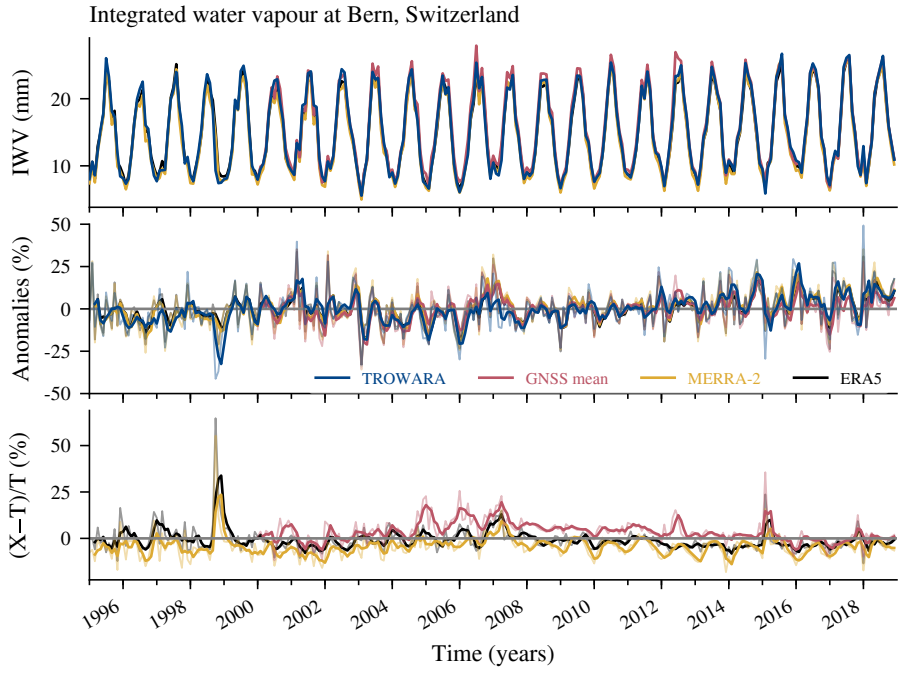

Figure 3. (a) Monthly means of IWV from the microwave radiometer TROWARA in Bern (Switzerland), from GNSS stations close to Bern, and from reanalysis grids (MERRA-2 and ERA5) at Bern. **(b)** Anomalies from the climatology ((data−climatology)/climatology) for each of the mentioned data sets. **(c)** Relative differences of the mentioned dataset X to TROWARA (T) data $((X - T)/T)$. The bold lines in **(b)** and **(c)** show the data smoothed with a moving window of three months, the thin pale lines show the unsmoothed monthly data.

https://doi.org/10.5194/acp-2020-77
Preprint. Discussion started: 24 February 2020

Atmospheric Chemistry and Physics Discussions

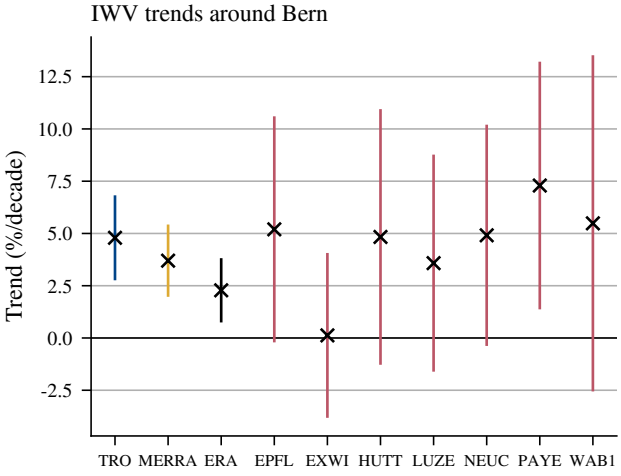

Figure 4. IWV trends for TROWARA (TRO) in Bern, reanalysis grids (MERRA-2 and ERA5) at Bern and GNSS stations close to Bern. The error bars show 2 σ uncertainties.

https://doi.org/10.5194/acp-2020-77
Preprint. Discussion started: 24 February 2020

Atmospheric Chemistry and Physics Discussions

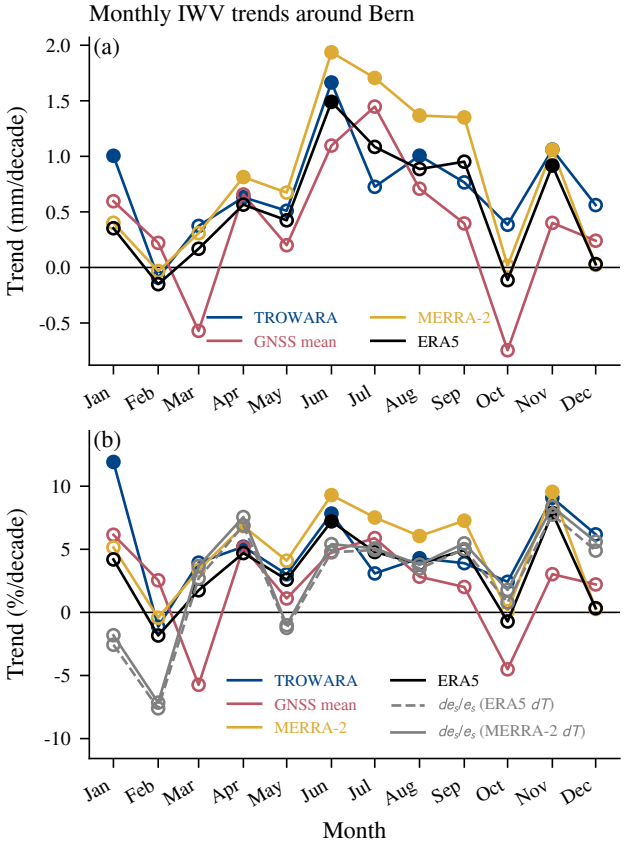

Figure 5. Trends of IWV for different months for TROWARA in Bern, GNSS stations close to Bern, and reanalysis grids (MERRA-2 and ERA5) at Bern. Panel **(a)** shows IWV trends in mm per decade. Panel **(b)** shows IWV trends in percent per decade and in addition the theoretical change in saturation vapour pressure e_s due to the observed temperature change from reanalysis data below $500\,\mathrm{hPa}$. Filled dots represent trends that are significantly different from zero at 95% confidence interval.

https://doi.org/10.5194/acp-2020-77
Preprint. Discussion started: 24 February 2020

Atmospheric Chemistry and Physics Discussions

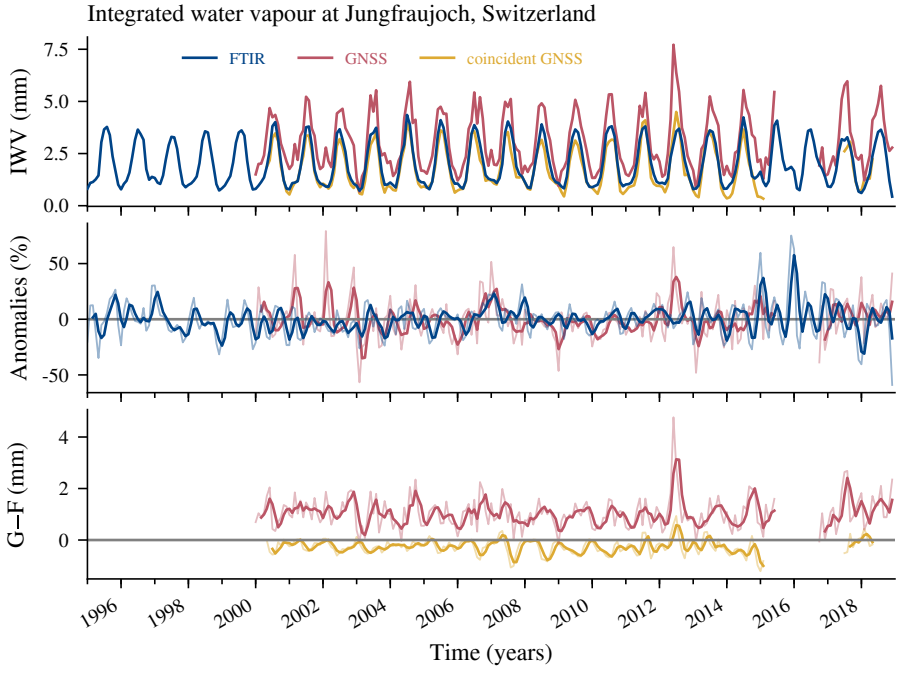

Figure 6. (a) Monthly means of IWV from the FTIR spectrometer and the GNSS station at Jungfraujoch (Switzerland). Shown are GNSS mohthly means once using the full hourly sampling and once using data only at the same time as the FTIR measured (coincident GNSS). The monthly means of FTIR and coincident GNSS have been resampled to correspond to the 15th of each month. **(b)** Anomalies from the climatology ((data−climatology)/climatology) for FTIR data and fully sampled GNSS data. **(c)** Differences between GNSS (G) and FTIR (F) data, using the full GNSS data and GNSS data coincident with the FTIR. The bold lines in **(b)** and **(c)** show the data smoothed with a moving window of three months, the thin pale lines show the unsmoothed monthly data.

https://doi.org/10.5194/acp-2020-77
Preprint. Discussion started: 24 February 2020

Atmospheric Chemistry and Physics Discussions

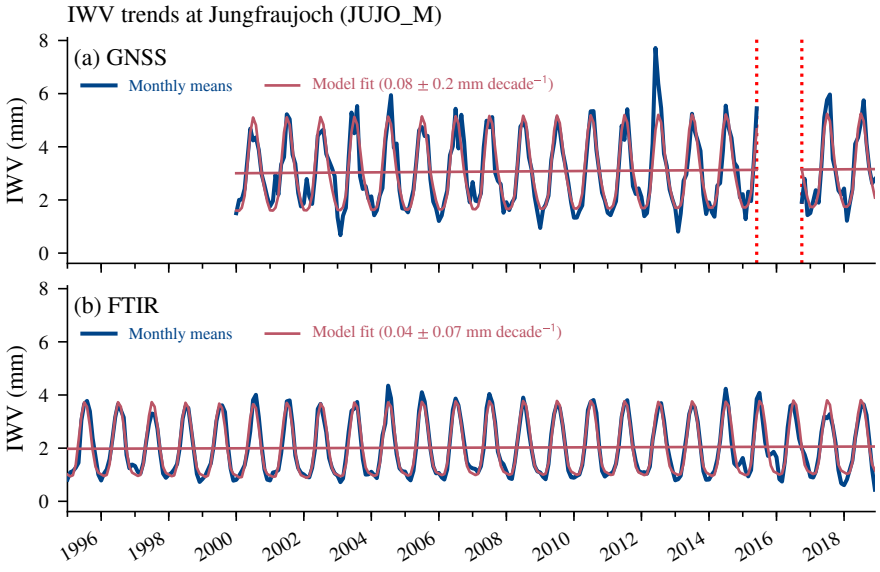

Figure 7. Monthly means and their trend fits for **(a)** GNSS and **(b)** FTIR data at Jungfraujoch. The given trend uncertainty corresponds to $2\,\sigma$ uncertainties. GNSS antenna changes are indicated by vertical red dotted lines.

https://doi.org/10.5194/acp-2020-77
Preprint. Discussion started: 24 February 2020

Atmospheric Chemistry and Physics Discussions

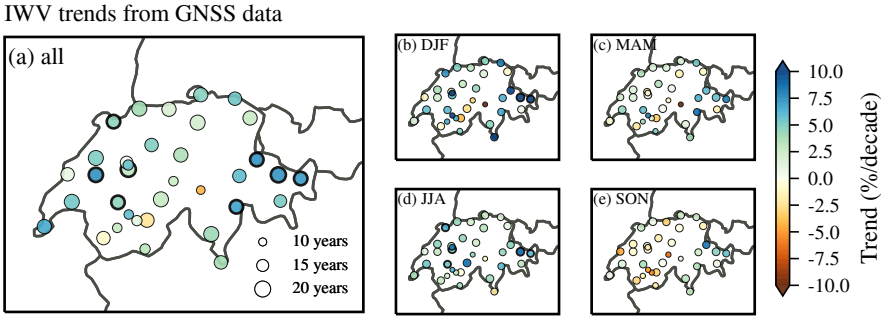

Figure 8. Trends of IWV in Switzerland for the different GNSS stations for the whole year **(a)** and the four seasons (**(b)** to **(e)**). The length of the GNSS time series (Table 1) is indicated by the size of the markers. Stations with trends that are significantly different from zero at 95% confidence interval are marked with a bold edge.

https://doi.org/10.5194/acp-2020-77
Preprint. Discussion started: 24 February 2020

Atmospheric Chemistry and Physics Discussions

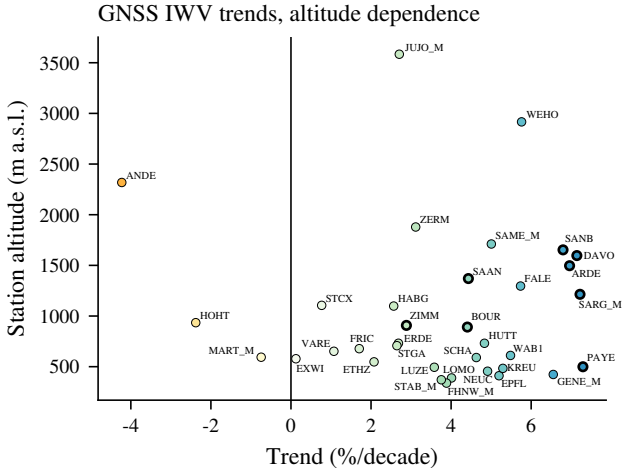

Figure 9. IWV trends from GNSS stations in Switzerland with the station altitude. For merged stations (see Table 1), the averaged altitude of both stations is used. The colors correspond to the trend in percent per decade and are the same as in Fig. 8. Trends that are significantly different from zero are shown with bold edges. The station abbreviations are explained in Table 1.

https://doi.org/10.5194/acp-2020-77
Preprint. Discussion started: 24 February 2020

Atmospheric Chemistry and Physics Discussions

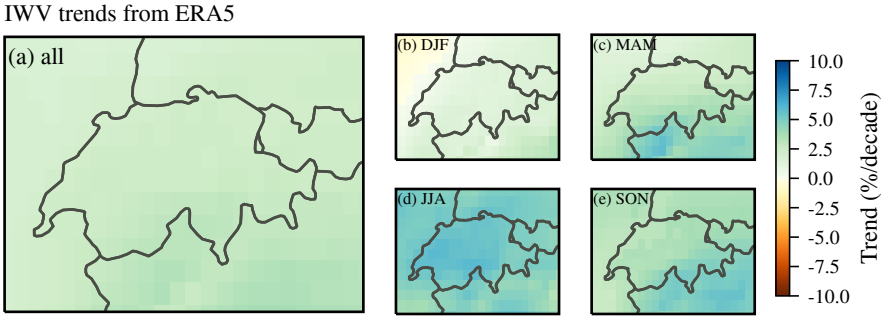

Figure 10. IWV trends from ERA5 reanalysis data in Switzerland from 1995 to 2018 for the whole year **(a)** and for the different seasons (**(b)** to **(e)**).

https://doi.org/10.5194/acp-2020-77
Preprint. Discussion started: 24 February 2020

Atmospheric Chemistry and Physics Discussions

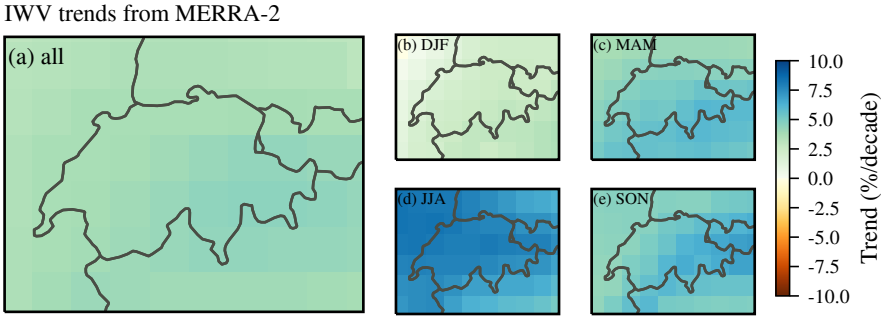

Figure 11. Same as Fig. 10 but for MERRA-2 reanalysis data (1995-2018).

https://doi.org/10.5194/acp-2020-77
Preprint. Discussion started: 24 February 2020

Atmospheric Chemistry and Physics Discussions

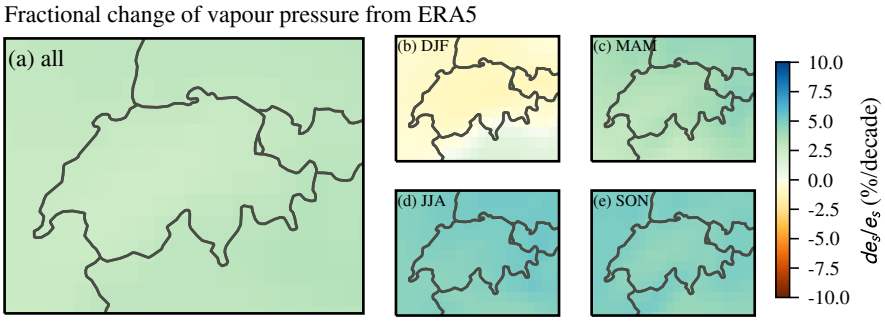

Figure 12. Fractional change of water vapour pressure (e_s) derived from temperature trends from ERA5 (1995-2018) for the whole year **(a)** and different seasons (**(b)** to **(e)**). The temperature data have been averaged below 500 hPa.

https://doi.org/10.5194/acp-2020-77
Preprint. Discussion started: 24 February 2020

Atmospheric Chemistry and Physics Discussions

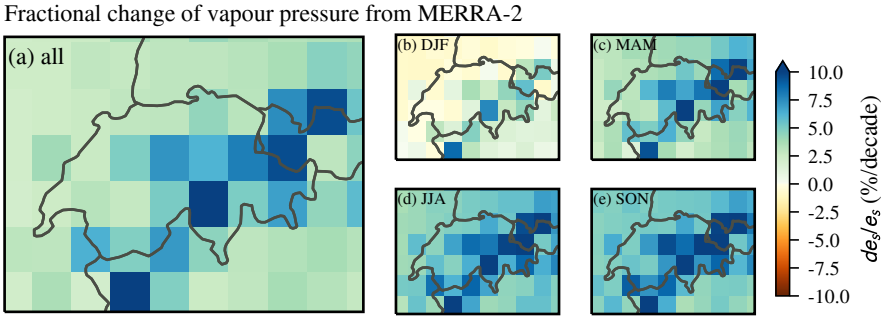

Figure 13. Same as Fig. 12 but using MERRA-2 temperature data averaged below 500 hPa (1995-2018).

https://doi.org/10.5194/acp-2020-77
Preprint. Discussion started: 24 February 2020

Atmospheric Chemistry and Physics Discussions

Table 1. Swiss GNSS stations used in the present study. Stations marked in bold were directly compared with radiometer and reanalysis data at Bern (latitutde = $46.95 \pm 0.5°$, longitude = $7.44 \pm 1°$, altitude = 575 ± 200 m).

Abbreviation	Station name	Altitude (m a.s.l.)	Data available	Remark
ANDE	Andermatt	2318	2000 to 2010	
ARDE	Ardez	1497	2002 to 2018	
BOUR	Bourrignon	891	2002 to 2018	
DAVO	Davos	1597	2000 to 2018	
EPFL	EPF Lausanne	411	2000 to 2018	
ERDE	Erde	731	2007 to 2018	No AGNES station
ETHZ	ETH Zurich	548	2000 to 2018	
EXWI	Exakte Wissenschaften Bern	578	2001 to 2016	No AGNES station
FALE	Falera	1296	2002 to 2018	
FHNW_M	Fachhochschule Nordwestschweiz Muttenz	347	2000 to 2018	Merged with FHBB (329 m) in 2018
FRIC	Frick	678	2001 to 2018	
GENE_M	Geneva	422	2001 to 2018	Merged with AIGE (424 m) in 2009
HABG	Hasliberg	1098	2007 to 2018	
HOHT	Hohtenn	934	2001 to 2018	
HUTT	Huttwil	731	2002 to 2018	
JUJO_M	Jungfraujoch	3584	2000 to 2018	Merged with JUJ2 (3585 m) in 2016
KREU	Kreuzlingen	483	2002 to 2018	
LOMO	Locarno-Monti	389	2000 to 2018	
LUZE	Luzern	494	2001 to 2018	
MART_M	Martigny	594	2002 to 2018	Merged with MAR2 (593 m) in 2008
NEUC	Neuchâtel	455	2000 to 2018	
PAYE	Payerne	499	2001 to 2018	
SAAN	Saanen	1370	2002 to 2018	
SAME_M	Samedan	1709	2003 to 2018	Merged with SAM2 (1712 m) in 2016
SANB	San Bernadino	1653	2002 to 2018	
SARG_M	Sargans	1211	2002 to 2018	Merged with SAR2 (1218 m) in 2011
SCHA	Schaffhausen	590	2001 to 2018	
STAB_M	Stabio	371	2002 to 2018	Merged with STA2 (371 m) in 2007
STCX	Saint-Croix	1105	2002 to 2018	
STGA	St. Gallen	707	2001 to 2018	
VARE	Varen	652	2006 to 2018	No AGNES station
WAB1	Wabern	611	2006 to 2018	No AGNES station
WEHO	Wetterhorn	2916	2007 to 2018	No AGNES station
ZERM	Zermatt	1879	2006 to 2018	
ZIMM	Zimmerwald	908	2000 to 2018	

https://doi.org/10.5194/acp-2020-77
Preprint. Discussion started: 24 February 2020

Atmospheric Chemistry and Physics Discussions

Table 2. IWV trends for TROWARA in Bern, GNSS stations close to Bern, and reanalysis grids (MERRA-2 and ERA5) at Bern, with $2\,\sigma$ uncertainties. Trends that are significantly different from zero at 95 % confidence interval are shown in bold. TROWARA and reanalysis trends are given for the period 1995 to 2018, GNSS trend periods are shown in Table 1.

Location	Data set	Trend (% per decade)	Trend (mm per decade)
Bern	TROWARA	$\mathbf{4.8 \pm 2.0}$	$\mathbf{0.72 \pm 0.30}$
Bern	MERRA2	$\mathbf{3.7 \pm 1.7}$	$\mathbf{0.53 \pm 0.25}$
Bern	ERA5	$\mathbf{2.3 \pm 1.5}$	$\mathbf{0.34, \pm 0.23}$
EPFL	GNSS	5.2 ± 5.4	0.84 ± 0.87
EXWI	GNSS	0.1 ± 3.9	0.02 ± 0.60
HUTT	GNSS	4.8 ± 6.1	0.70 ± 0.88
LUZE	GNSS	3.6 ± 5.2	0.58 ± 0.84
NEUC	GNSS	4.9 ± 5.3	0.78 ± 0.84
PAYE	GNSS	$\mathbf{7.3 \pm 5.3}$	$\mathbf{1.14 \pm 0.93}$
WAB1	GNSS	5.5 ± 8.0	0.95 ± 1.39